Development of high density magnetic recording media for hard disk drives: materials science issues and challenges

G. W. Qin*[1], Y. P. Ren[1], N. Xiao[1], B. Yang[1], L. Zuo[1] and K. Oikawa[2]

The tremendous increase in areal density of hard disk drives is mainly ascribed to harmonic development between magnetic recording media and heads in their scaling, especially allowing a commercial transition from the longitudinal to perpendicular recording system. This paper reviews the main features, recent breakthroughs and future potentials of both the longitudinal and the perpendicular media from a viewpoint of materials science. Special attention is firstly paid to the 'trilemma' problem for the media, i.e. the compromise among writability, thermal stability and signal to noise ratio (SNR). The evolution of media materials these years are then addressed with emphasis on the thermodynamic origin of magnetically induced phase separation of Co–Cr based alloys, which governs media noise and coercivity, and its applications to the current longitudinal media. The materials challenges for media to achieve 500 Gb in.$^{-2}$ and above are further predicted from the viewpoints of thermal stability improvement and microstructure control of media materials, and their engineering issues have been discussed for the current Co–Cr based alloys, potential FePt and CoPt ordered, phase separated Co–W based alloys and magnetic rare earth compounds. Finally, the future media approaching 1 Tb in.$^{-2}$ and beyond are addressed with respect to the principles, progress, engineering challenges and future directions.

Keywords: Magnetic recording media, Longitudinal recording, Perpendicular recording, Magnetically induced phase separation, Grain size scaling, Texture, Review

List of symbols and acronyms

a	the transition width
A	the exchange stiffness constant
AAO	alumina anodic oxidisation
AD	areal density
B	the bit length
BPM	bit patterned media
BER	bit error rate
CGC	continuous granular composite media
D	the bit diameter or in-plane grain size of media
d	the head to media spacing
d_{ss}	the spot size of light in HAMR
$\mathrm{d}H_C/\mathrm{d}T$	the medium coercivity dependence of temperatures
$\mathrm{d}T/\mathrm{d}x$	the spatial gradient of temperature in the medium heated by the local incident light
erfc	the complementary error function
f_0	the attempt frequency ($\sim$1 GHz)
fcc	face centred cubic structure
g	the head gap
${}^0G_i$	the Gibbs energy of one pure phase
${}^EG_m$	the excess Gibbs free energy expressing the deviation from the ideal behaviour of solution
${}^{mag}G_m$	the magnetic contribution, which is a function of composition, temperature and structure
GMR	giant magnetoresistance
GPM	granular perpendicular media
h_{ex}	the exchange field
H_C^{max}	the maximum coercivity of media allowing magnetic head to write
H_K	the anisotropy field of media
H_{SW}	the critical switching field for a coherent switching in the model of Stoner–Wolfarth (SW)
HAMR	heat assisted magnetic recording
hcp	hexagonal closed packed structure
HDD	hard disk drive
k_B	the Boltzmann's constant
KV	the magnetic anisotropy energy, where K is the magnetic anisotropy constant and V is the grain volume
M_r	the remanent magnetisation

[1]Key Laboratory for Anisotropy and Texture of Materials (Ministry of Education), Northeastern University, Shenyang 110004, China
[2]Graduate School of Engineering, Tohoku University, Sendai 985-0875, Japan

*Corresponding author, email qingw@smm.neu.edu.cn

Published by Maney for the Institute and ASM International
DOI 10.1179/174328009X411172

M_S^{head}	the saturation magnetisation of the pole
M_S	the saturation magnetisation of media
MIPS	magnetically induced phase separation
n	the refractive index of media
PW_{50}	the full width at half maximum of the readback voltage pulse
s	the cross-track correlation length
s_D	bit spacing in BPM
SFD	switching field distribution
SNR^{total}	the total SNR, including the transition SNR (SNR^{trs}) and the DC SNR (SNR^{DC})
SNR	signal to noise ratio
SUL	soft magnetic underlayer
T	the absolute temperature
X_i (i=Co, Cr, Z)	the mole fractions of Co, Cr and Z elements respectively
w	the track width
α	the relation coefficient of the transition width a
α_d	the damping constant for GPM
β	the ratio of the write track width to the bit length
β_e	the extent of the intergranular exchange coupling
γ	the ratio of PW_{50} to B
δ	the medium thickness
θ	the angle between the easy axis and the applied field
θ_L	half of the angle of the marginal light
λ	the wavelength of the incident light
σ	the in-plane area distribution of grains
σ_{s_D} and σ_D	the standard deviations of bit spacing and diameter in BPM respectively

Introduction

It was reported that the annual data storage capacity in the world reached 5×10^{10} GB in 2002, which is about 800 MB per year per person, roughly doubled compared to that in 1999.[1] This huge amount of data is stored in commercial information storage media, which can be classified into four categories depending on the storage techniques, namely, the optical storage (such as CDs, VCDs and DVDs), the semiconductor storage (such as Flash memories and SD cards), the magnetic–optical storage (MO disks) and the magnetic storage (such as magnetic tapes, floppy disks and hard disk drives).

Among the four data storage techniques, the hard disk drives (HDDs) of the magnetic storage exhibit the highest areal density and data transfer rate so far, usually several to hundreds of times those of the other three techniques in both important performances above, and thus play an important role in the current data storage industry and also daily life of people.[1] It is expected that the annual products of HDDs will reach 5×10^6 in 2009.[2]

The progress in HDDs is astonishing so far; however, the original HDD could be dated to IBM350 RAMAC (Random Access Method of Accounting and Control)

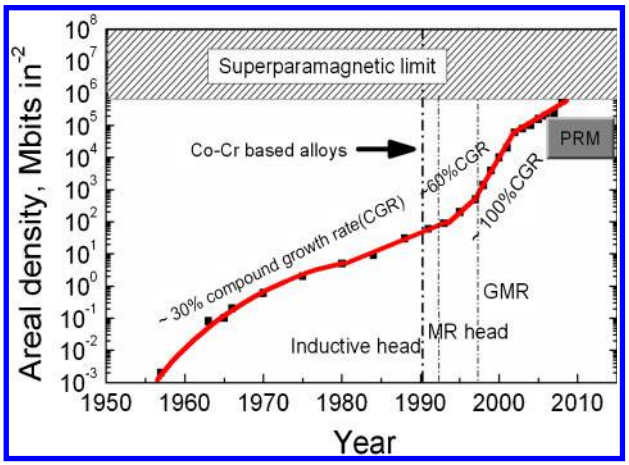

1 Areal density roadmap of HDD media in the last five decades with an increase of over 300 million times, experiencing inductive head,[1–4] magnetoresistive (MR) head and GMR head, and Co–Cr based alloy thin films since the 1990s, and perpendicular recording media (PRM) commercially available since 2006 but now suffering from a bottleneck limited by the superparamagnetism of the present media

invented in 1957 with an areal density of only 2 kb in.$^{-2}$. Owing to the rapid development, especially during the past one decade, the demonstrated areal density has reached 610 Gb in.$^{-2}$ in 2008,[3] i.e. increased by more than 300 million times over the past 50 years, as shown in Fig. 1.

The rapid increase in the areal density of HDDs enables product miniaturisation and also cost reduction. The absolute price per megabyte has been lower than that of printed papers since 1996.[4] This tremendous increase in the areal density has extended many applications of HDDs, not only the well known computer hard disk memories, but also the other consumer electronics, such as video cameras, high capacity cell phones, home servers and so on.

Such a great achievement in the areal density of HDDs is due to successful development of both magnetic head and media, two important components of HDDs, since, as we know, the harmonic development between the two components has made a major contribution. One of the breakthroughs in the head technique is the introduction of the giant magnetoresistance (GMR) technique since 1996, of which the main contributors Professor A. Fert and Professor P. Grünberg were awarded the Nobel Prize in physics in 2007. Generally speaking, the magnetic head technique experienced inductive heads, magnetoresistive heads, anisotropic magnetoresistive heads and GMR (or future tunnelling magnetoresistive) heads in the past several decades, as shown in Fig. 1. A detailed review on the magnetic heads is out of the scope of this paper, but can be found elsewhere.[5,6]

Owing to the limit of the paper length, this review does not cover many important aspects of HDDs, such as abovementioned head technology, head flying control, signal detection, tracking control and so on. The fundamental physics issues of media can be found in a recent review by Richter.[7] Instead, the present review will focus on the evolution of materials science and processing of media for HDDs, and challenges in the

future. Special attention is paid to the magnetic materials and engineering for the development of high density magnetic recording media, including materials design, microstructure and texture control, and also their correlation with the magnetic properties of media.

A brief introduction to the fundamental magnetism of recording media will be first addressed in the section on 'Fundamental magnetism of magnetic recording media', including the writing limit, signal to noise ratio (SNR), thermal stability of recorded bits in both the widely used longitudinal recording media and the newly established perpendicular recording media. The important parameters of media materials will be deduced for the media design of current optimisation and future developments. The section on 'Media materials evolution' introduces the media materials evolution of recent years in both the longitudinal and the perpendicular media. Much attention will be paid to the thermodynamic origin of magnetically induced phase separation in the current Co–Cr based alloy media, which governs media noise and coercivity, in particular in the longitudinal media, and its thermodynamic mechanism will be discussed in detail as well as the effects of important additives, such as Pt, Ta and B, to improve the magnetic properties of media. The material challenges for media to achieve 500 Gb in.$^{-2}$ are predicted from the viewpoints of the thermal stability improvement and microstructural control consideration (e.g. grain size, size distribution, texture and so on), and their engineering breakthroughs and challenges will be introduced in the section on 'Materials science challenges for media to achieve the areal density of 500 Gb in.$^{-2}$ and above'. The section on 'Future media beyond 1 Tb in.$^{-2}$' gives the media with the potential of 1 Tb in.$^{-2}$ and beyond. The magnetic materials issues on percolated perpendicular media (PPM), bit patterned media (BPM) and heat assisted magnetic recording (HAMR) are highlighted, including their main principles, recent progress, engineering challenges and future directions. The paper ends with a short summary with an expectation that a hybrid technology combining those proposals above will be feasible to reach an areal density of 1 Tb in.$^{-2}$ and beyond.

Fundamental magnetism of magnetic recording media

The schematics of the magnetic recording modes are shown in Fig. 2. The longitudinal recording mode, which has been used for several decades, writes signals into media along the media plane, storing the magnetisation of each bit lying in the media plane. In contrast, the perpendicular recording mode records each bit normal to the film plane, and thus the magnetisation of each bit is either 'up' or 'down'. Even though the areal density of HDDs has increased tremendously, the recording principles have not changed so much in nature. Generally speaking, the two recording modes follow the same basic principles. Such a tremendous increase in the areal density is contributed by the miniaturisation of head, the improvement of reading sensitivity and the optimisation of media materials, which have been indeed guided by some fundamental magnetics and other physical considerations. Step by step improvements of physical background and relevant

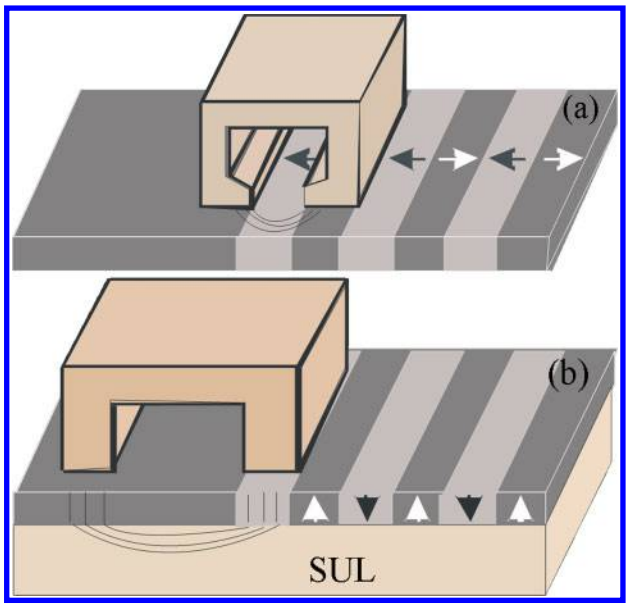

2 Schematics of magnetic recording geometry: *a* longitudinal recording in single magnetic layer and *b* perpendicular recording in a magnetic layer with a keeper (soft magnetic underlayer, SUL)

technologies and sometimes, big breakthroughs of magnetic materials, have made the areal density limit shift from initial 10 Gb in.$^{-2}$ (about 10 years ago)[8] to 100 Gb in.$^{-2}$,[7,9–11] and to presently predicted 500–1000 Gb in.$^{-2}$.[12–14]

In principle, three aspects are usually considered for the fundamental magnetic performances of media: writing limit, SNR for signal reading and thermal stability of recorded bits, among which they are balanced and constrained one another.[7–16] First, SNR is practically important for signal processing. To store a bit signal with a sufficiently high SNR, a volume of a bit recorded in the media must include an adequate number of magnetic grains. That is, the smaller the grain sizes, the higher the areal density is. However, excessively small grains tend to confront a serious problem, the superparamagnetic limit which depends on a magnetic anisotropy energy constant K of the medium material. For a grain with a size smaller than the limit, the magnetic anisotropy energy KV (V is the grain volume) is overcome by the thermal agitation energy k_BT (k_B is the Boltzmann's constant and T is the absolute temperature), resulting in the thermal decay of magnetic memory sustained by the grains. Generally, the storage of information in one medium must be secured for 10 years for industrial applications. In other words, the value of KV should be larger than $60k_BT$. In order to keep the sufficient SNR against the rapid increase in bit density, media materials of higher anisotropy are needed to allow downsizing of the magnetic grains. The increase in anisotropy will result in higher media coercivity when the grains are well isolated. It is finally limited by the writability of a magnetic head. These problems in the trilemma, and therefore, should be considered carefully for the development of media.

Writing limit

The writing limit corresponds to a limit of the maximum field generated by a head to write signals into media. Hence, the medium should have a right coercivity in

order to be magnetised by the magnetic head field, i.e. the writing field. Actually, the maximum writing field depends on the geometry of a head, recording mode and the saturation magnetisation of the pole M_S^{head}. To avoid saturation close to the head gap, the gap field is generally assumed to be 80% of the value of $4\pi M_S^{head}$. On the other hand, the media coercivity for longitudinal recording should be less than 40% of the applied field to perform perfect writing.[15–17]

For the longitudinal recording mode, as shown in Fig. 2*a*, when one considers the head efficiency, the maximum coercivity of media H_C^{max} can be accordingly deduced as follows[17]

$$H_C^{max} = 0{\cdot}20 \times 4\pi M_S^{head} \tan^{-1}\left(\frac{g/2}{d+\delta}\right) \quad (1)$$

where g is the head gap, d is the head to media spacing and δ is the medium thickness. Assuming that the head to media spacing is close to 5 nm, representing the state of art level, and that the maximum saturation magnetisation of a head is 2·4 T, the maximum coercivity dependence on the media thickness and the head gap was calculated using equation (1) and summarised in Fig. 3*a*. With decreasing medium thickness, the medium tends to be magnetised by a weaker field, but for a given medium thickness, it becomes harder for a head with a smaller gap to magnetise the medium properly. That is, a lower coercivity medium is preferred for higher density longitudinal recording. For a higher coercivity medium, its thickness should be thinner to be right magnetised.

By the same token, we can calculate the maximum coercivity of media for the perpendicular recording mode. Assuming that the easy axis of each magnetic grain is normal to the film plane with perfect orientation and considering the demagnetisation field, one can get an allowable coercivity H_C^{max}, modified by the equation as[5]

$$H_C^{max} = 0.8 \times 4\pi M_S^{head} \times \tan^{-1}\langle (TW/4)/\left\{(d+\delta)[(T/2)^2+(W/2)^2+(d+\delta)^2]^{1/2}\right\}\rangle - 4\pi M_S d/(d+\delta) \quad (2)$$

where M_S is the saturation magnetisation of media, and T and W are the pole thickness and track width (or the pole width) of the main pole of a head respectively. The dependence of the maximum coercivity on the medium thickness and the track width in the perpendicular recording is thus calculated using equation (2), as shown in Fig. 3*b*. In contrast to the longitudinal recording, the perpendicular recording geometry can generate a much higher field, while the medium thickness has a similar effect on the writing field to that in the longitudinal media. The geometry of the single pole head has a significant effect on the writing field, which is increased by increasing either pole thickness or track width, as shown in Fig. 3*b*.

At the same time, the smaller the throat height of the main pole, the higher the generated writing field is. In addition, the writing field and thus the tolerant maximum medium coercivity can be further increased if the keeper layer (that is, soft underlayer) is used. But the saturation magnetisation and thickness of the soft underlayer (SUL) have a weak effect on the writing field, i.e. the resulted writing field will approach to a saturated value when the SUL thickness is over than 50–100 nm.[5,6]

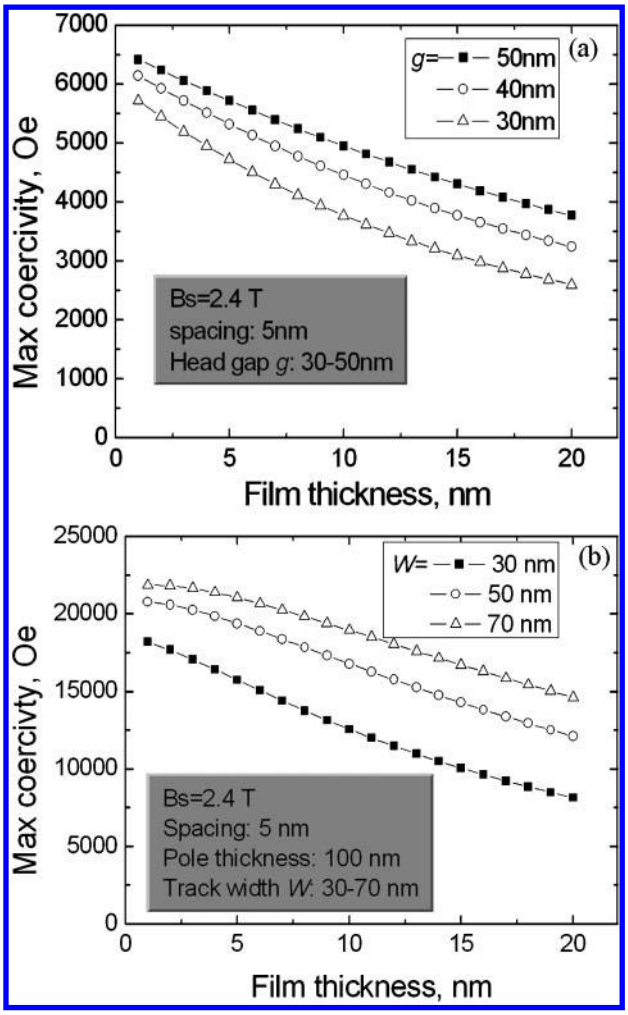

3 The tolerant maximum coercivity of media dependent on the media thickness available by the sufficient magnetisation of a head, assuming the head saturation flux density of 2·4 T and the head to media spacing of 5 nm: *a* longitudinal recording and *b* perpendicular recording

In the calculation for perpendicular media, the demagnetisation field is considered as $4\pi M_S d/(d+\delta)$. It decreases with increasing thickness of the magnetic layer. Its effect can be negligible, in particular for the relative low M_S media, when the medium thickness is more than two times the head to media spacing, as shown in Fig. 3*b*. But, note that the media thickness should not be beyond a critical value δ_C, at which the magnetisation reversal changes from the coherent rotation mode to the incoherent one (curling). This critical thickness has been determined both experimentally and theoretically. Theoretically, it is[7,18]

$$\delta_C = 4(AK^{-1})^{1/2} \quad (3)$$

where A is the exchange stiffness constant and K is the magnetic anisotropy of media. For a typical case, $A \approx 10^{-6}$ emu cm^{-1} and $K = 6 \times 10^6$ emu cm^{-3}, then equation (3) yields $\delta_C \approx 16$ nm.

Figure 3*b* shows that perpendicular recording permits media with higher anisotropy and coercivity than those of the longitudinal recording. It is very instructive for

the grain downsizing and the improvement of SNR in the perpendicular media. On the other hand, according to the angle dependence of the writing field, tilted media would allow a much lower writing field or a higher medium coercivity.[19] The critical switching field H_{SW} for a coherent switching in the model of Stoner–Wolfarth (SW) is given as

$$H_{SW} = H_K\left[(\cos\theta)^{2/3} + (\sin\theta)^{2/3}\right]^{-3/2} \quad (4)$$

where H_K is the anisotropy field of media and θ is the angle between the easy axis and the applied field. The switching field shows the minimum at θ=45°, that is, a tilted media with an easy axis deviated 45° from the film normal will allow the lowest writing field for the perpendicular media.

Signal to noise ratio

Signal to noise ratio (SNR) is a measure of the readback voltage strength relative to the background noise, and is one of the practically important parameters determining the error rate of HDD systems and thus the final areal density limit. Generally, the noise of HDD system includes playback amplification noise arising from the fluctuations of current or voltage, the head noise due to the loss impedance and the media noise caused by the fluctuation of magnetisation of bits and their interaction. Among which, the first two types of noise have a weaker effect on the SNR than the media noise in the current HDD systems. For the details, please refer to Bertram's book.[20] The media noise is mainly composed of DC noise and transition one. The DC noise, or particulate noise, is a direct consequence of the granularity of the media, which produces a variance of the magnetisation and signal amplitude with grain diameter and grain orientation variations. The transition noise is generated by the transition region and increases linearly with the transition density $\sim 1/\pi a$, which is determined mainly by intergranular exchange coupling and magnetostatic interaction, where a is the transition width between the two neighbouring bits. Therefore, the total SNR (SNR^{total}) includes the transition SNR (SNR^{trs}) and the DC SNR (SNR^{DC}) can be written as[11,21]

$$\frac{1}{SNR^{total}} = \frac{1}{SNR^{trs}} + \frac{1}{SNR^{DC}} \quad (5)$$

$$SNR^{DC} = 1{\cdot}85\frac{wPW_{50}}{s^2(1+\sigma)}\frac{M_r^2}{\Delta M^2}$$

$$\left(\Delta M^2 = <M_x^2> - M_r^2\right) \quad (6)$$

$$SNR^{trs} = \frac{96}{\pi^5}\frac{wB}{s(1+\sigma)}\frac{PW_{50}}{a^2} \quad (7)$$

where w is the track width, PW_{50} is the full width at half maximum of the readback voltage pulse, B is the bit length, s is the cross-track correlation length, M_r is the remanent magnetisation and σ is the in-plane area distribution of grains. Equations (5)–(7) show that SNR is very sensitive to remanent magnetisation and its distribution, grain size and its distribution as well as intergranular exchange coupling for a given bit size. If the intergranular exchange coupling is negligible, then s can be roughly assumed to be equal to the magnetic grain size. If the transition noise is dominant in high density recording media, the system error rate (PE for a PR4 channel) can be expressed by[15,16]

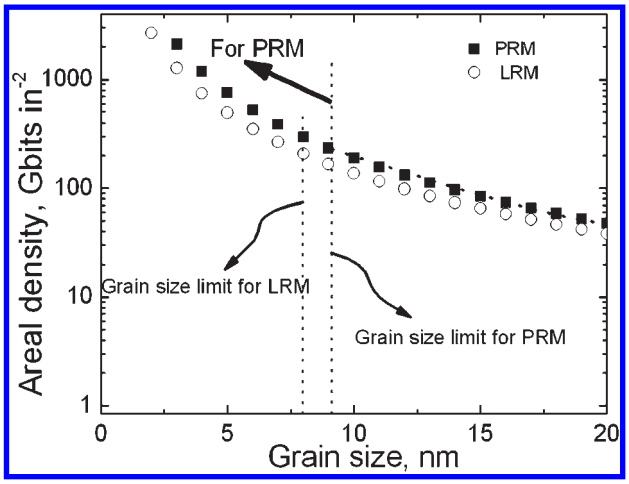

4 The areal density dependence on the in-plane grain size for both the longitudinal and perpendicular media. The grain size limits are also given for the two recording modes assuming H_K=15 000 Oe, film thickness of 15 nm and SNR=22 dB for 10 years

$$PE = 0{\cdot}5\,\mathrm{erfc}\left[\frac{\pi^{1/2}}{6}\left(\frac{SNR}{\gamma}\right)^{1/2}\right] \quad (8)$$

where erfc is the complementary error function, and γ is the ratio of PW_{50} to B. Then the areal density AD dependent on SNR/γ is written by Bertram as follows[16]

$$AD^{3/2} = \frac{0{\cdot}28\beta}{\alpha^2 D^3(1+\beta)^{3/2}(SNR/\gamma)(1+\sigma)} \quad (9)$$

where β is the ratio of the write track width to the bit length and α is the relation coefficient of the transition width a depending on the recording modes,[16,21,22] that is

$$\alpha \approx 0{\cdot}5 + 6\frac{M_S}{H_K}e^{-(d+\delta/2)/5D}\ln\left[1+\left(\frac{\delta}{4D}\right)e^{(d+\delta/2)/D}\right]$$

(for longitudinal recording) (10)

$$\alpha = \left[(1/\pi)^2 + 0{\cdot}35(a_{WC}/D)^2\right]$$

(for perpendicular recording) (11)

where a_{WC} is the 'Williams–Comstock' transition width. In the longitudinal recording, equation (10) is valid for two-dimensional randomly oriented media, negligible head field rising time, $d+\delta/2 \leqslant 3{\cdot}5D$, $\delta \leqslant 2{\cdot}0D$ and $M_S/H_S \leqslant 0{\cdot}10$ (in CGS).[21] If the head field rising effect is considered, the α value should be modified as suggested by Middleton and Miles.[22]

It is obvious that the SNR strongly depends on the grain size, grain in-plane area distribution, areal density and saturation or remanence magnetisation, which will be discussed in the following section. The areal density dependence on the magnetic grain size is thus calculated using equations (5)–(11) considering the correlation of SNR to areal density, as shown in Fig. 4, for a medium of the anisotropy field of 15 000 Oe and SNR of 22 dB which is assumed to last for 10 years. The areal density increases drastically with decreasing grain size, especially in the region below 10 nm. Both the longitudinal and

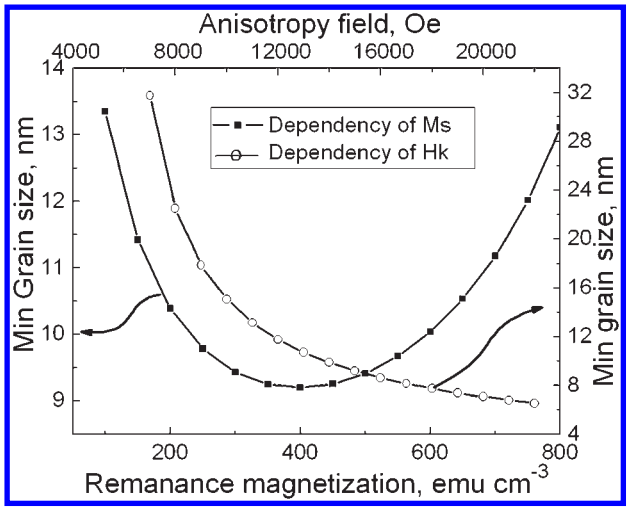

5 The grain size limit dependence on either anisotropy field or remanence in the case of perpendicular medium with a thickness of 15 nm

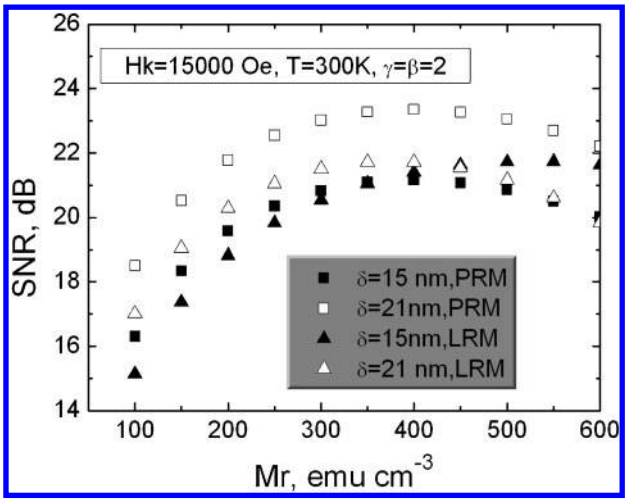

6 SNR correlation with the remanence for the two recording modes at room temperature for 10 years, assuming H_k=15 000 Oe, δ=15 nm and $\gamma=\beta=2$

perpendicular media can attain a maximum density of about 200 Gb in.$^{-2}$ due to the limit of thermal stability of recorded bits. However, for the perpendicular recording media, the grain size limits can be further reduced by increasing the media anisotropy field, whereas it is very difficult for the longitudinal recording media, if not impossible.

Thermal limits

After writing, the recorded bits are subjected to thermal fluctuation at a certain temperature. Thus, the remanence magnetisation of the recorded bits decays with time. The decaying rate depends strongly on the magnetic anisotropy energy and volume of grains as well as temperature. If the thermal decay follows a general Néel–Arrehnius's rule and a half of remanence is detectable during a certain period t, then the reversal energy barrier ΔE can be expressed by[16]

$$\Delta E = k_B T \ln(t f_0 / \ln 2) \tag{12}$$

where f_0 is the attempt frequency ($\sim$1 GHz), k_B is the Boltzmann's constant ($1{\cdot}38\times10^{-16}$ erg K^{-1}) and T is the temperature. If the magnetostatic field is considered, the energy barrier for the longitudinal and perpendicular media will be expressed by[16]

$$\Delta E = \frac{\pi}{8} H_K M_S D^2 \delta \left\{1 - 16 M_r \delta \left[\left(1+4\beta^2\right)^{1/2} - 1\right] [\mathrm{AD}(1+\beta)]^{1/2}/\beta\right\}^{3/2} \quad (\text{for LRM}) \tag{13}$$

$$\Delta E = \frac{\pi}{8} H_K M_S D^2 \delta (1 - 4\pi M_S/H_K)^2 \ (\text{for PRM}) \tag{14}$$

Combining equations (12) and (13) or (14), the grain size limit can be evaluated for the two recording media, which were already shown in the literature.[16,23]

Assuming H_K=15 000 Oe, β=2, δ=15 nm and SNR=22 dB for 10 years, the grain size limit is estimated to be about 8 nm for the longitudinal recording and about 9 nm for the perpendicular recording, as shown in Fig. 4. It is hard for the longitudinal recording to further downsize the grains beyond $\sim$200 Gb in.$^{-2}$, while there is still some room for the perpendicular recording. Our calculation verified that the grain size limit has a strong correlation to the remanence (or saturation) magnetisation, as shown in Fig. 5. One optimised magnetisation of $\sim$400 emu cm^{-3} is to achieve the smallest grain size, and the grain size can be further reduced to 6 nm or less if the anisotropy field or the magnetic anisotropy constant is further increased. In this case, it will be possible to attain a higher density of 500–600 Gb in.$^{-2}$ with a reasonably decayed SNR of 22 dB for 10 years.

Figure 6 shows that the decayed SNR for 10 years has a much stronger correlation to the film thickness in the perpendicular recording than that in the longitudinal recording, which is calculated by combining equations (9)–(14). The longitudinal recording media have almost the same maximum SNR, independent on the film thickness, but the product of remanence × thickness varies little, which has already been confirmed by both theory and experiments.[16] However, it has a different shape for the perpendicular recording. Increasing the medium thickness from 15 to 21 nm results in an SNR increase by about 2 dB. This means that the grains with a high aspect ratio (height to in-plane diameter ratio) are preferred for the perpendicular recording to achieve a higher SNR or areal density.[7]

Media materials evolution

Since the 1980s, Co–Cr based alloys have been regarded as the only feasible alloy system for media of HDDs. During the past two decades, the study on the Co–Cr based alloys was focused on the Co–Cr binary alloys in the 1980s, but extended to the Co–Cr–Pt and Co–Cr–Ta alloys in the 1990s, and to the Co–Cr–(Pt, Ta, B) for the longitudinal recording media and Co–Cr–Pt–SiO_2 metal oxide granular films for the perpendicular media in the 2000s. Then, an essential question should be addressed, i.e. why all of the media are based on the Co–Cr alloy system. In addition to a good corrosion resistance due to the addition of Cr, the system has the other two merits:

(i) a sufficiently high magnetocrystalline anisotropy energy
(ii) phase separation induced by intrinsic magnetic ordering.

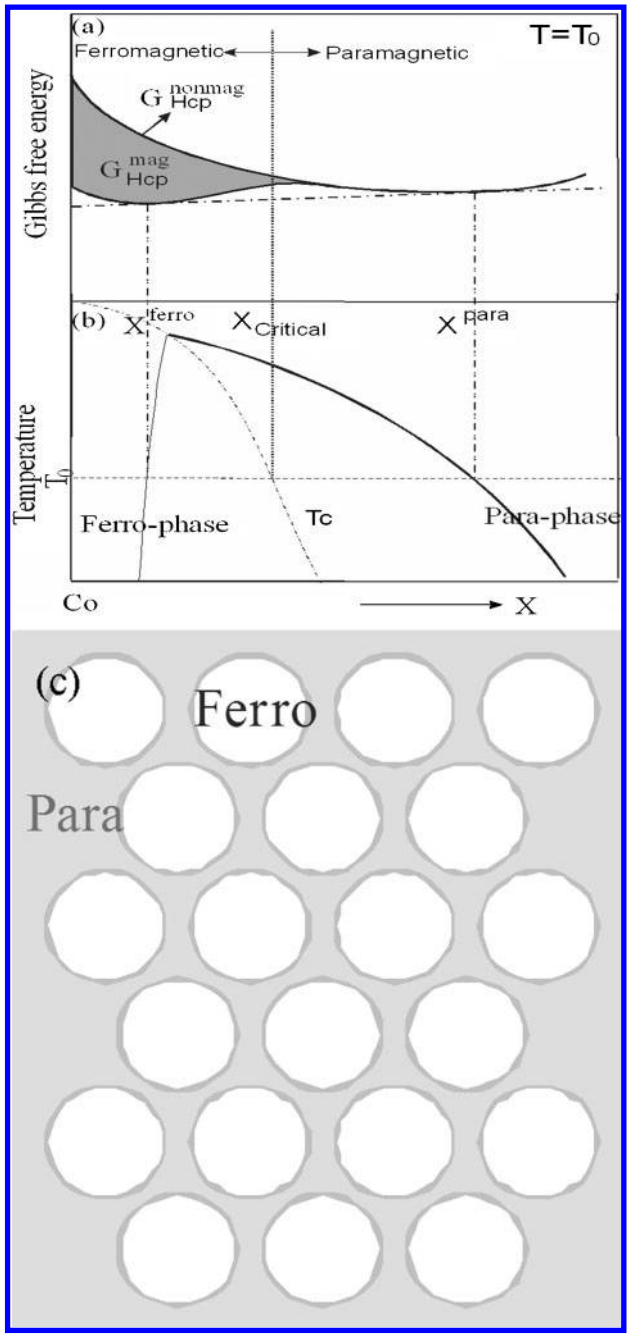

7 Sketches of magnetically induced phase separation: *a* Gibbs free energy *v.* concentration X at a certain temperature T_0, *b* corresponding Co–X binary phase diagram and *c* resulted two-phase microstructure, i.e. ferromagnetic and paramagnetic phases

The high magnetic anisotropy arises from the hexagonal closed packed (hcp) structure of cobalt, and can be enhanced by the addition of Pt, which has been well documented.[24,25]

In the following, much attention is paid to the specific microstructure of the Co–Cr based alloy films, that is, the nanosized Co rich ferromagnetic phase is surrounded by the Cr rich paramagnetic phase, as shown in Fig. 7. The well defined isolation is due to the spontaneous decomposition of the alloy film during sputtering, and with this microstructure, the media transition noise is greatly reduced. This particular two-phase microstructure played a major role in development of the Co–Cr based media, responsible for the increase in the SNR and also the areal density in the 1990s–2000s. Hasebe *et al.* theoretically predicted the magnetically induced phase separation (MIPS) in the Co rich corner at high temperature (fcc structure) of Co–Cr system as early as in 1982, that is, fcc structured Co rich and Cr rich phase in the Co–Cr system.[26] Later, the two-phase microstructure (hcp structure) of the Co–Cr thin films was observed in 1985 by Maeda *et al.*[27] However, there was lack of experimental data to support Hasebe's prediction at that time and it was thus hard to correlate the MIPS to the hcp structured two-phase microstructure of the Co–Cr thin films. In 2000, Qin *et al.* experimentally confirmed the MIPS in the bulk Co–Cr alloys and then thermodynamically reassessed the Co–Cr binary system.[28] Finally, these results were used to explain some phenomena related to Co–Cr thin films which had been debated for a long time,[28] and thus concluded that the MIPS was responsible for the two-phase microstructure, that is, hcp structured Co rich and Cr rich phases in the sputtered Co–Cr thin films.

Thermodynamic origin of magnetically induced phase separation of Co–Cr alloys

Magnetically induced phase separation, on which typical experiments of Fe–Cr–Co alloys performed by Kaneko *et al.* in 1971[29] and theoretical calculation performed by Nishizawa *et al.* in 1979,[30] implies that Gibbs free energy of alloys in one composition range rapidly decreases due to the intrinsic magnetic ordering at a given temperature T_0, resulting in the curve shape of Gibbs free energy *v.* concentration from 'one valley' to 'two valleys', that is, 'W' shaped Gibbs free energy curve, as shown in Fig. 7*a*. One alloy within the certain concentration range is, therefore, unstable, and decomposes into the two phases rather than keeping the original one-phase state. This kind of phase separation happens always along the Curie temperature line, as shown in Fig. 7*b*, and resulting in the two-phase microstructure for these alloys (Fig. 7*c*) within this composition gap, named the miscibility gap.

For the Co–Cr binary alloy system, however, its reliable phase diagram in the Co rich corner was not known until the end of the 1990s.[26,28,31] Because of the low diffusivity of the Co–Cr alloys, it is hard to experimentally measure the corresponding phase diagram at that time, even though the thermodynamic model had already been proposed[26,30] and confirmed for the other magnetic alloy systems.[29,30,32] Qin *et al.* experimentally verified that the MIPS happens in a high temperature face centred cubic (fcc) structure phase region in the Co–Cr binary system, and further deduced from the point of view of thermodynamics that it should also be available for the metastable hcp structure experiencing a similar MIPS as the stable fcc structure at high temperatures,[28] as shown in Fig. 8. Actually, the diffusivity of the Co–Cr alloy in the process of sputtering deposition should be much larger than that of bulk case since the sputtering provides higher kinetic energy of the deposited atoms to move on a substrate surface, especially at high substrate temperatures. Consequently, a faster phase separation is attainable in the sputtering deposition process than an annealing process of the bulk alloys.

In Fig. 8, the predicted metastable miscibility gap well explains the thermomagnetic data, nuclear magnetic

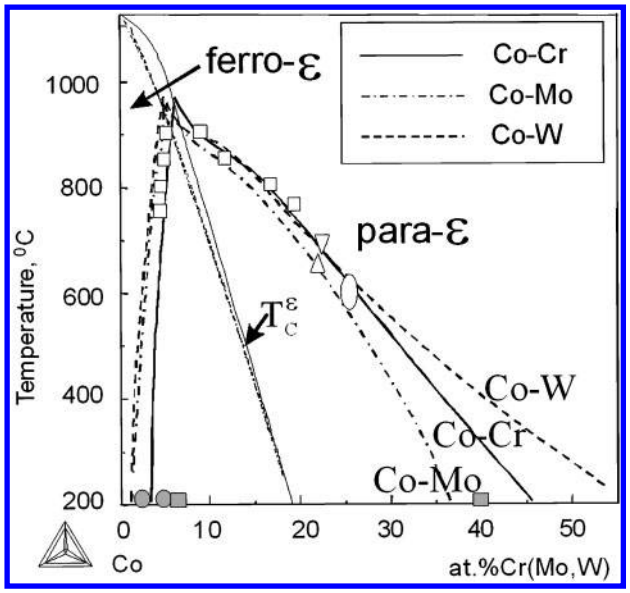

8 The calculated metastable miscibility gaps of the hcp structured (ε) Co–X (X=Cr, Mo, W) systems, and experimental data for the Co–Cr system are incorporated for comparison (Ref. 28 and references therein), fcc structured ferro-/paraphase equilibrium data (□), thermomagnetic data of hcp structure (△▽○), NMR data of hcp structure (●) and atom probe analysis on hcp structure (■)

resonance (NMR) data and atom probe analysis on a series of the Co–Cr alloys by many groups (Ref. 28 and references therein), confirming that the two-phase microstructure is due to the MIPS indeed. In this figure, Co–W and Co–Mo binary systems were also predicted to have a similar MIPS as the Co–Cr system, which will be discussed in more detail later.

Application of MIPS model to current design of media materials

Since the two-phase microstructure in the Co–Cr based recording media is governed by the MIPS, it is possible to modify compositions of the decomposed two phases by designing Co–Cr–Z ternary or multicomponent systems, and thus to tailor the exchange coupling among the magnetic grains, especially for longitudinal recording media. For a given width of grain boundary phase, for instance, Cr rich phase in Co–Cr based longitudinal media, its Curie temperature should be lower than room temperature to ensure its paramagnetic state at the ambient temperature and thus to ensure good exchange decoupling. Therefore, small addition of some alloying elements which contribute to enrichment of the Cr and/or alloying elements themselves in the Cr rich phase will benefit the exchange decoupling. Oikawa *et al.* classified the effects of the third additives on the Co–Cr alloy system, and qualitatively concluded that various elements, such as B, Nb, Pd, Pt, Ta, Zr and so on, are expected to expand the miscibility gap.[33] With the addition of these elements, the Cr content in the paramagnetic phase is largely increased, thus decoupling magnetic grains in the media. Here, the important work is summarised to clarify the effect of Pt, Ta and B additives in the current magnetic recording media.[34,35]

Thermodynamic model

The subregular solution model describes the molar Gibbs free energy of the hcp phase in a Co–Cr–Z ternary system as

$$G_m = X_{Co}{}^0G_{Co} + X_{Cr}{}^0G_{Cr} + X_Z{}^0G_Z + RT(X_{Co}\ln X_{Co} + X_{Cr}\ln X_{Cr} + X_z \ln X_z) + {}^EG_m + {}^{mag}G_m \quad (15)$$

where X_i (i=Co, Cr, Z) is the mole fraction of Co, Cr and Z elements respectively, and ${}^0G_i$ is their Gibbs energy of one pure phase. Here the excess Gibbs free energy ${}^EG_m$ expresses the deviation from the ideal behaviour of solutions. The magnetic contribution ${}^{mag}G_m$ is a function of composition, temperature and structure, which is well described.[36]

Co–Cr–Pt ternary system

The Co–Pt is a completely miscible system in the hcp state in the Co rich corner, and the miscibility gap in the Co rich corner of the Co–Cr–Pt ternary system is thus obtained,[34] as shown in Fig. 9*a*. A small addition of Pt ($<\sim$10 at.-%) broadens the ternary miscibility gap to some extent, but with further addition, the miscibility gap becomes narrower and terminates on the Co–Pt side along the Curie temperature line. At the same time, the Pt addition ($>\sim$10 at.-%) shifts the gap to the Co rich side obviously. As a result, the Cr content in both the ferro- and paramagnetic phases decreases.

For the Co–Cr binary alloy media, the Cr content of the Cr rich phase should be larger than 20 at.-% to ensure its paramagnetic state at ambient temperature and thus to exchange decouple the magnetic grains. However, the Cr content of the Cr rich phase usually varies among about 15–25 at.-% for typical Co–Cr based longitudinal media containing 12–18 at.-%Cr. It means that some grains cannot be well decoupled when the Curie temperature of the corresponding Cr rich phase is higher than room temperature or the content of non-magnetic elements is not high enough, especially for the its Cr content lower than 20 at.-%. So the increase in Cr content of the Cr rich phase and its width (volume) will benefit exchange decoupling of the magnetic grains.

From the calculation result of Co–Cr–Pt isothermal section at 400°C (Fig. 9*a*), it can be seen that a small addition of Pt ($<\sim$10 at.-%) significantly expands the miscibility gap. According to the level's rule, the volume (or width for a given thickness of medium) of the Cr rich phase decreases very slightly in this case. However, its Cr content increases obviously, that is, the proper addition of Pt contributes to enrichment of Cr in the Cr rich phase, thus decoupling of magnetic grains. In other words, the probability of magnetic Cr rich grain boundary phase decreases at ambient environment. At the same time, the Cr content of the Co rich phase decreases with addition of Pt, and it can thus be predicted that the anisotropy energy of the Co rich phase will be improved with the addition of Pt into the Co–Cr alloys due to a synergetic effect of both addition of Pt itself and decrease in Cr in the Co rich phase. This is consistent with the experiments by Ikeda *et al.*[37] Kitakami *et al.*[38] experimentally found that the Pt addition enhances the magnetic anisotropy energy of Co–Cr based media, which supported our calculation, too. From Fig. 9*a*, it can also know that the miscibility

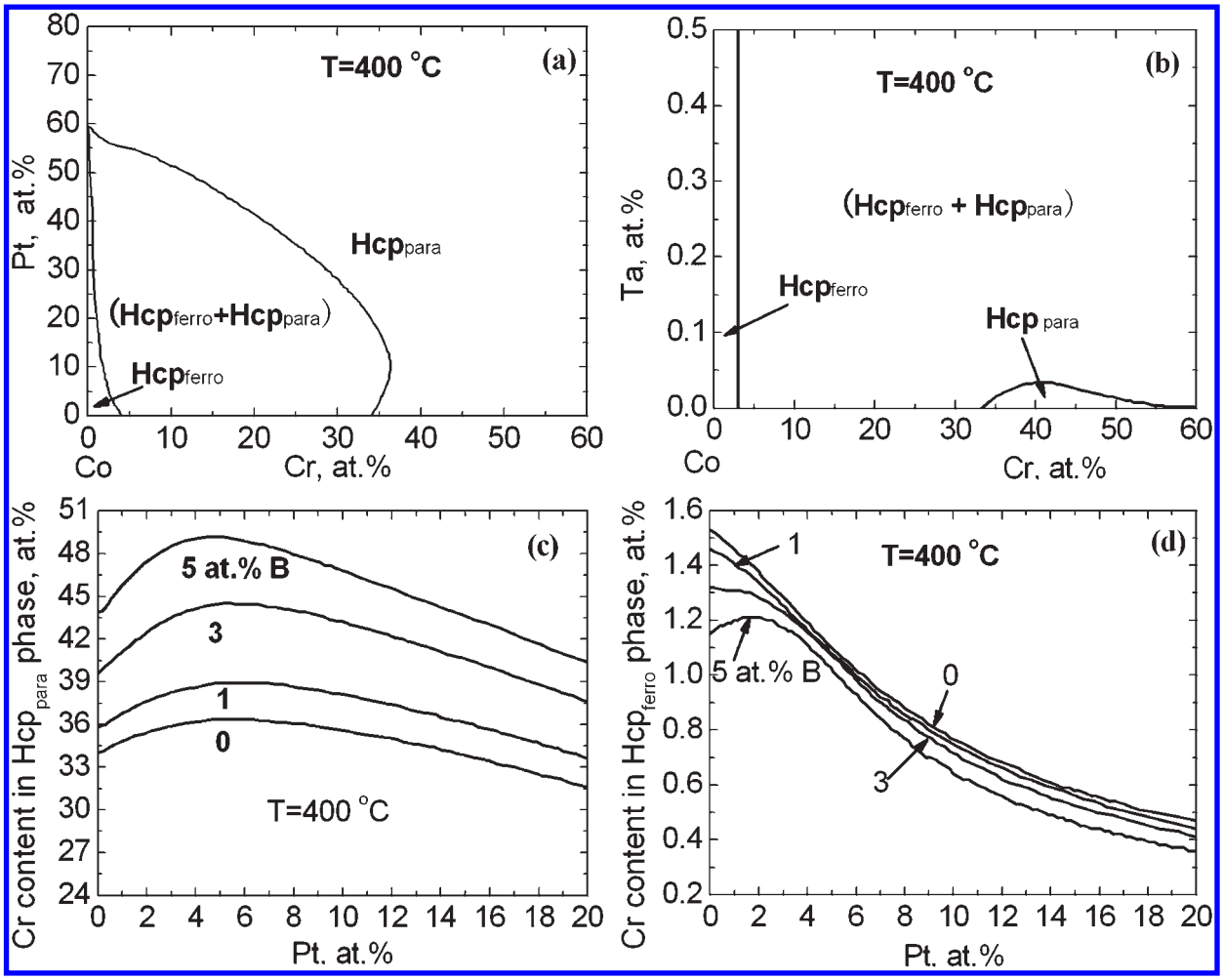

9 The calculated isothermal sections of the Co–Cr–Z (Z=Pt, Ta, B) systems at 400°C, showing effects of additives on the shape of metastable miscibility gap in the Co rich corner of these systems: *a* Co–Cr–Pt;[34] *b* Co–Cr–Ta[40] and *c*, *d* Co–Cr–Pt–B[35]

gap becomes narrower and obviously shifts the gap to the Co rich side when the Pt addition is larger than ~10 at.-%, that is, the recording noise becomes larger for the Co–Cr based media with the Pt content larger than 10 at.-%. Inaba *et al.*[39] reported that the Cr segregation is reduced by the addition of 13 at.-%Pt, i.e. the Pt addition deteriorates the SNR of the Co–Cr based media. These experimental results are in good agreement with our thermodynamic predictions, and it is thus verified that the thermodynamic calculation is a useful tool to understand the processing–microstructure–magnetic property relationships of the Co–Cr based longitudinal recording media.

Co–Cr–Ta ternary system

Figure 9*b* shows an isothermal section of the Co–Cr–Ta system at 400°C.[40] The solubility of Ta in the ε-Co phase is very limited, and the Cr content in the ferromagnetic phase varies little with the small addition of Ta, while that in the paramagnetic phase increases dramatically. This calculation predicts that the Ta addition will improve the final recording noise (transition noise). The experimental results by Inaba *et al.*[39] and Hirayama *et al.*[41] showed that the Cr segregation is enhanced in the Co–Cr–Ta media, which supports our calculation again.

Co–Cr–Pt–B quaternary system

The longitudinal recording media in the 2000s are usually based on the Co–Cr–Pt–B quarternary alloy system, which shows a sufficiently high magnetic anisotropy and higher SNR due to the addition of Pt and B.[42,43] Based on the calculation of the Co–Cr–Pt ternary system,[34] Oikawa *et al.* further verified the effect of boron in the Co–Cr–Pt ternary system,[35] as shown in Fig. 9*c–d*. With the addition of boron, the Cr content of the paramagnetic phase significantly increases while that of the ferromagnetic phase decreases. It can be thus predicted that the intergranular exchange coupling is decreased, and that the magnetic anisotropy should be improved at the same time. These predictions are in good agreement with the experimental results that the addition of boron facilitates the intergranular exchange decoupling[42] and accordingly, decreases the media noise.[43] It can also be known that the coaddition of Pt and B should be more effective to improve the magnetic anisotropy and recording noise than the addition of Pt or B alone. The optimised composition can be easily gotten via the calculation results, also evidenced by experiments.[44]

Materials science challenges for media to achieve areal density of 500 Gb in.$^{-2}$ and above

Magnetically induced phase separation (MIPS), as discussed above, plays a dominant role in governing the intergranular exchange decoupling of media, and

thus, both the SNR and the areal density increase, particularly for the longitudinal media. In order to further increase the areal density up to 500 Gb in.$^{-2}$ and above, it is becoming more important to improve the thermal stability of the recorded bits, magnetic grain isolation, texture control and engineering grain size in the media to achieve higher SNR.

Thermal stability improvement

High SNR is indispensable for ultrahigh density recording, which is approximately proportional to the grain numbers in each bit,[45] as discussed in the section on 'Fundamental magnetism of magnetic recording media'. In this case, a serious problem, the superparamagnetic effect, arises when the magnetic grains are further downsized. Here we summarise five proposals which have been addressed so far to improve the thermal stability of the recorded bits.

The first one is the antiferromagnetically coupled media, proposed by Fujitsu and IBM in 2000 for longitudinal recording and commercially available since then.[46,47] The key point of this technique is to introduce a very thin interlayer Ru (0·6–1·0 nm), 'Pixie dust', between the two hard layers, resulting in the lower layer antiferromagnetically coupled to the upper one via indirect exchange coupling. The resultant energy barrier maintains or enhances the thermal stability of the media as compared to the single layer media, and the remanence thickness product is the difference between them. This kind of design has advantages not only for the thermal stability improvement, but also for the decrease in the transition parameter a and thus for increase in the linear density. The SNR in this case is comparable to the previous single layer media because both the signal and noise are the difference between the two layers when the two layers are antiparallel grain by grain.[48] Otherwise, the noise would be enhanced, yielding poor SNR. For the detailed review, please refer to the literature.[46–48]

The second way to improve the thermal stability is to change the recording mode from the longitudinal to the perpendicular. The perpendicular recording was proposed by Professor S. Iwasaki in 1978,[49] and its advantage is obvious for nanometre scale recording, especially allowing a medium with much higher coercivity, as calculated in Fig. 3*b*. For a given anisotropy energy material, it is easy to understand that the thermal stability, or energy barrier, can be improved by the grain shape modification, i.e. the high aspect ratio grains. The perpendicular recording prefers this microstructure rather than the longitudinal recording because of the linear density limit, demagnetisation effect and the exchange coupling effect, as discussed in the section on 'Fundamental magnetism of magnetic recording media'. The maximum SNR is kept at a rough constant of the remanence thickness product, and any increase in the medium thickness for the longitudinal media will be compromised by the intergranular exchange coupling related to the composition and size dependent MIPS.

It should be noted that the thickness in the perpendicular recording is also limited by the magnetisation reversal mode, which have been discussed in the section on 'Fundamental magnetism of magnetic recording media'. Moreover, the demagnetisation field in the current perpendicular mode is comparable to that in the longitudinal mode, especially for the media thickness between 10 and 20 nm. So the priority in the thermal stability aspect is somewhat limited for the perpendicular recording if the demagnetisation effect is considered. While the perpendicular media can give very perfect orientation and very narrow distribution of the media anisotropy due to the paramagnetic oxide isolation, both of them contributes to a higher SNR gain.[7] For the longitudinal media, the magnetic isolation arises from the MIPS of the media themselves. The media have a large fluctuation of Cr either at grain boundaries or inside grains, resulting in a wider switching field distribution and thereby, SNR loss. The commercial and research communities are changing their interest from the current longitudinal to the perpendicular media because, also, several potential recording techniques, such as hard/soft exchange spring media or composite media, heat assisting recording media, BPM and so on, are all based on the perpendicular recording mode, which will be discussed later.

The third method to improve the thermal stability is to engineer the higher order term of the magnetic anisotropy constants. Theoretical work has been addressed by Bertram and Safonov,[50] Peng and Richter[51] and Kitakami *et al.*[52] to verify this issue. For an intrinsic anisotropy energy density E of media, $E=K_1\sin^2\theta+K_2\sin^4\theta$, where K_1 and K_2 are the first order and second order anisotropy constants respectively. For a perpendicular medium, the K_2 term plays a dominant role in increasing the thermal stability without changing the switching field. With increasing ratio of $K_2K_1^{-1}$ to about 0·4, the energy barrier is doubled while the switching field increases little.[52] The similar fact happens for the longitudinal media, but it is effective only when the media with easy axis is well oriented to the applied field, usually the deviation angle less than 27°.[51] In this case, thermal stability benefitted from the K_2 term cannot be countered by the media writability.

Much work so far has suggested feasibility of engineering the anisotropy terms K_1 and K_2.[53–55] For a given medium, K_2 usually increases with decreasing K_1, but the ratio of the $K_2K_1^{-1}$ is significantly affected by seedlayers.[55] The series of seedlayers, such as Cu, Ir, Au, Pd, Pt, Ru and Re, were chosen to verify this effect by Sato *et al.* using the Co–25Pt alloy media, and the results showed that the Pd and Pt seedlayers contribute to high K_1 and K_2, and also high $K_2K_1^{-1}$ ratio. They argued that these changes to the growth modes of the different seedlayers since the lattice parameters of the Co–Pt layer did not monotonically increase with that of the seedlayers.[55] A further study should be performed to clarify this mechanism, but the results are instructive for engineering K_1 and K_2 for novel media design.

The fourth way to improve the thermal stability is based on composite media, or called 'hard/soft exchange spring media', 'domain wall assisted media' or 'exchange coupled media'. If the hard layer is ferromagnetically coupled with the soft layer, it can drastically decrease the switching field without deterioration of thermal stability. Suess *et al.* calculated that the energy barrier could be significantly improved doubly by adjusting the thickness ratio of the hard/soft layer.[56] Both the two spin model[57,58] and the spin chain model[59] have been used to illustrate the exchange spring media, and some useful conclusions have been obtained as follows: the

soft layer with a positive anisotropy will facilitate the hard layer to switch rather than that without the anisotropy; the strongest composite effect happens for an optimum magnetisation thickness product ratio between the two layers; an optimum exchange coupling exists between the ferromagnetically coupled layers. For the detailed discussion, please refer to the literature by Richter.[7]

The fifth method to improve thermal stability is the use of high magnetic anisotropy materials. It is easy to understand, since any increase in the anisotropy energy permits to downsize grains, and many materials with high magnetic anisotropy are available up to date, especially for the perpendicular recording. In this case, the intergranular exchange decoupling among grains, realised by the MIPS in the longitudinal media, can be tailored by the cosputtered oxides such as Al_2O_3 or SiO_2. Here we classify all the investigated potential alloys so far into four types

(i) modification type based on the currently used Co–Cr–Pt alloys
(ii) phase separation type based on Co–Mo(W) alloys
(iii) ordering type based on FePt and CoPt alloys
(iv) rare earth (RE) compound type, such as $SmCo_5$, NdFeB and so on.

In the longitudinal media, Co–Cr–Pt based alloys with high Cr content (10–20 at.-%) and low Pt content (5–15 at.-%) are widely used to achieve a sufficient high anisotropy and good MIPS. Composition modification can significantly increase the magnetic anisotropy, such as via decreasing the Cr content and increasing the Pt content.[53,55] From the thermodynamic calculations, the MIPS is obviously suppressed if the Cr content is lower than $\sim$10 at.-%. On the other hand, if the Pt content is larger than 25 at.-%, the fcc structured phase appears with a much lower anisotropy, which is not desired for ultrahigh density recording.[60] An alternative way to solve the insufficient MIPS problem in the case of the lower Cr content is to introduce an oxide to form granular media, particular for the perpendicular media, which has been well documented.[53–55,61] One has to keep in mind that the magnetic anisotropy decreases to some extent with the addition of SiO_2 because the silicon and/or oxygen are included in the magnetic grains more or less during sputtering processing.[53] Even so, the local compositions inside each grains or at grain boundaries in the granular perpendicular media are more homogeneous than in the MIPS typed longitudinal media. The homogeneity in composition usually results in a narrow distribution of both the anisotropy and the remanence, and thus contributes to a high SNR.[7]

The magnetic anisotropy could also be improved by optimising the magnetic layer thickness and seedlayers.[55,60] With decreasing thickness of the magnetic layer, the magnetic anisotropy generally increases, but the increase depends strongly on underlayers and seedlayers.[55,60] One possible explanation says that it is due to the misfit induced effect between the magnetic layer and the underlayer.[55,60] Experimental results soundly confirm it since the value of *c*/*a* of the magnetic layer is significantly changed with different misfits.[60] However, the answers are still welcome to the question why seedlayers play different roles in the case of a similar misfit.

Phase separation type alloys refer to the Co–Mo(W) based alloys, proposed by Oikawa *et al.*[62,63] It has been shown that the magnetic anisotropy of the Co–Mo(W) alloys is much higher than that of the corresponding Co–Cr alloys. Moreover, both the thermodynamic calculation and the experiments confirm that there is a similar MIPS indeed as in the Co–Cr alloy media,[62,63] as shown in Fig. 8. For these two reasons, the two alloy systems were suggested to be promising materials for the potential recording media. Unfortunately, the MIPS in the two systems is somewhat limited as compared to the Co–Cr system.[63,64] The Mo(W) content at the grain boundaries is not high enough to exchange decouple the magnetic grains in media, leading to high noise and low coercivity. Qin *et al.* clarified that this insufficient phase separation may be due to the elastic energy arising from the coherent misfit between the decomposed two phases, and lower diffusivity than that of the Co–Cr alloy system.[64] Any attempt is interesting to improve their intrinsic MIPS by optimisation of alloying or processing in the future without deterioration of their anisotropy energy density.

Ordered FePt and CoPt alloys are promising materials for future media owing to their sufficient high magnetic anisotropy ($(5\times10^7$–10×10^7 erg cm^{-3}).[11,65] However, their ordering temperatures are as high as 500–700°C during sputtering or post-annealing, thus setting a barrier to their applications for the time being.[11] Many attempts have been conducted to decrease the ordering temperatures, and proper alloying is an effective way.[66–70] Ag,[66] B,[67] Sn and Pb[68] are effective additives to decrease the ordering temperatures of the CoPt films, to as low as $\sim$350°C, and Ag, Au[69] and Zr[70] are effective for the FePt films. An alternative way was also proposed to decrease the ordering temperatures through, such as Fe/Pt multilayers and postannealing,[71,72] and proper underlayers.[73] The other key point of the application of the FePt and CoPt ordered films is to control perfect [001] texture, which is one of the main contributions to the high SNR and can be controlled by either epitaxial growth[74,75] or non-epitaxial growth.[76]

As one possible future media beyond 500 Gb in.$^{-2}$, the nanosized grains of the ordered CoPt or FePt phase should be tunably isolated. In this case, however, their coercivities are much high, usually larger than several tens of thousands of Osters,[75] completely out of the head writability, as discussed in the section on 'Fundamental magnetism of magnetic recording media'. In order to decrease the coercivity of FePt alloys, Suess *et al.*[77] suggested FePt/Fe_3Pt/FePt trilayer structured medium. With increasing thickness of the interlayer Fe_3Pt, the coercivity is obviously decreased while the energy barrier is further improved. Okamoto *et al.* found that the capping layer of Pt has also a significant effect on decreasing the coecivity.[78] They explained an induced magnetisation in the capping Pt layer and thus had a similar exchange spring effect, finally contributing to the coercivity decrease but without deterioration of the thermal stability.

Nanoscale size dependence of long range ordering has been confirmed in both discontinuous FePt thin films[79] and FePt–Al_2O_3 granular films,[80] where the critical size is about 3–4 nm. The FePt grains are hard to be ordered if the sizes are less than the critical size. Actually the surface and/or interface energy should seriously affect

the ordering of FePt when the particles size is less than 10 nm. Under these circumstances, the quantity of the surface and/or interface energy is comparable to the chemical free energy of a given nanoparticle. Takahashi *et al.*[80] calculated the size dependence on the ordering using the diffuse interface theory,[81] and got a consistent conclusion with their experimental observations. Yang *et al.*[82] studied this ordering transformation by the Monte Carlo method and supported the above conclusions. Okamoto *et al.*[83] further experimentally verified the dependence of magnetic properties on the ordering parameter, and concluded that the first order anisotropy constant K_1 gradually increases with the ordering parameter of the FePt films but weak (little) dependence of the Curie temperatures (and yet the K_2 constant).

The interfacial defects, antiphase boundaries (APB), appear in the FePt nanograins and should be taken into account. Since the local structure symmetry is broken for each FePt nanograin, the magnetic anisotropy may be degraded. Miyazaki *et al.*[79] found size dependence of the APB in the FePt nanograins, mostly existing in the grains with size larger than $\sim$4 nm. They suggested that a high substrate temperature deposition might overcome this problem to some extent.

Rare earth compounds, proposed as future recording media, have been paid relatively little attention up to now,[84–89] possibly owing to their much high magnetic anisotropy (for example, $Fe_{14}Nd_2B$, $4{\cdot}6\times10^7$ erg cm^{-3}; $SmCo_5$, $1{\cdot}1\times10^8$–2×10^8 erg cm^{-3})[11] and their poor oxidation resistance as well as their poor crystallisation at common sputtering conditions. Generally speaking, higher magnetic anisotropy of media allows smaller magnetic grains to be against the thermal energy, and thus benefit higher theoretical areal density. However, the medium coercivity is usually higher than 20 000 Oe when the smaller magnetic grains are isolated for the medium with a magnetic anisotropy energy density at magnitude of 10^7 erg cm^{-3}, for example, isolated and ordered FePt nanoparticles film,[75] which is completely out of the present writing ability of magnetic head. For the ordered FePt media with a similar magnetic anisotropy to $Fe_{14}Nd_2B$, this problem could be overcome by either FePt/Fe_3Pt/FePt trilayer structured medium,[77] capping layer of Pt on FePt layer[78] or control of ordering parameters,[79] as discussed above. However, there is little work up to date that a similar method is available for the magnetic RE compounds.

On the other hand, these magnetic RE compound media are usually amorphous in structure at low sputtering temperatures owing to their complex structures, and thus the high substrate temperatures, over than 300°C, are necessary for both the $SmCo_5$ and NdFeB alloy films to achieve good crystallisation. It is not applicable for industrial mass production, and the fatal problem is also for their poor oxidisation resistance at high temperatures. A proper capping layer is an effective way to solve this problem, but certainly increases the head medium spacing.

Even so, there have been some interesting results on this topic.[84–89] $SmCo_5$ was initially suggested to be a longitudinal medium and the proper Cr underlayer induced in-plane easy axis, but with a small coercivity of $<$2 kOe.[84] Sayama *et al.* later found that the suitable underlayer Cu can induce very perfect perpendicular anisotropy and Ti seeding layer further increases out-of-plane coercivity as high as 12 kOe and decreases minimal stable magnetic grain size as small as $\sim$4 nm.[85] The perpendicular anisotropy of the $SmCo_5$ can be ascribed to the Cu interdiffusion leading to the $Sm(Co,Cu)_5$ formation, thus facilitating the crystallisation and preferred orientation.[86] The Ru buffer layer is necessary to suppress the interdiffusion when the Co based soft underlayer is used. Unfortunately, the strong exchange coupling among the grains leads to a much large magnetic cluster size over than 100 nm.[86]

Tungsten was found to be a proper underlayer for NdFeB films with the perpendicular anisotropy,[87,88] and the maximum coercivity achieved was as high as 9·7 kOe.[88] But many dislocations and soft phases appear when the NdFeB layer thickness is over than 30 nm.[87] In order to further decrease the magnetic grain size and also exchange coupling, the addition of aluminium is an effective way, decreasing grain size down to $\sim$10 nm.[89]

Isolation of magnetic grains

The intergranular exchange coupling in media is one of the very important parameters determining the SNR and thus the areal density for both perpendicular and longitudinal recording.[1,2,7,11] Generally speaking, the exchange coupling increases remanence magnetisation but decreases coercivity, namely, it increases squareness of the demagnetisation curve. The exchange coupling also improves the thermal stability of recorded bits but the strong exchange coupling usually results in much loss of the SNR.[90]

As discussed in the section on 'Media materials evolution', the magnetic grain isolation is an essential way to decouple magnetic grains, through the MIPS for the longitudinal media and the oxides isolation for the perpendicular media. The MIPS occurs always at high substrate temperatures, usually at 200–300°C in the case of the commercial longitudinal media.[11] However, it is hard for the perpendicular media to keep both the perfect orientation and the grain isolation at high temperatures. Usually, a low deposition temperature benefits the perpendicular orientation, but suppresses the MIPS. In this case, oxides, typically SiO_2, are introduced to tune the exchange coupling among magnetic grains, as shown schematically in Fig. 10. Another advantage of introduction of SiO_2 is to provide a less deviation of remanent magnetisation and anisotropy than MIPS type media, and it thus contributes to a higher SNR and areal density. This arises from different thermodynamic features between SiO_2 and Co based alloys, resulting in homogeneous composition distribution of SiO_2 along grain boundaries of Co based nanograins during sputtering. However, the disadvantage of introduction of SiO_2 is that Co based nanograins contain a little Si and O after sputtering, and thus seriously decrease the magnetic anisotropy energy of these magnetic nanograins.[53]

The exchange field h_{ex}, in many simulation cases, is usually expressed by $h_{ex}=AK^{-1}D^{-2}$ (Refs. 91–93), where K is the anisotropy constant, A is the exchange stiffness and D is the in-plane grain size including the isolated grain boundary width. Here it should be pointed out that A is not a constant but proportional to the grain size, and thus the exchange field is inversely proportional to the grain size D rather than D^2.[7] For example, if the grain size changes from 10 nm down to

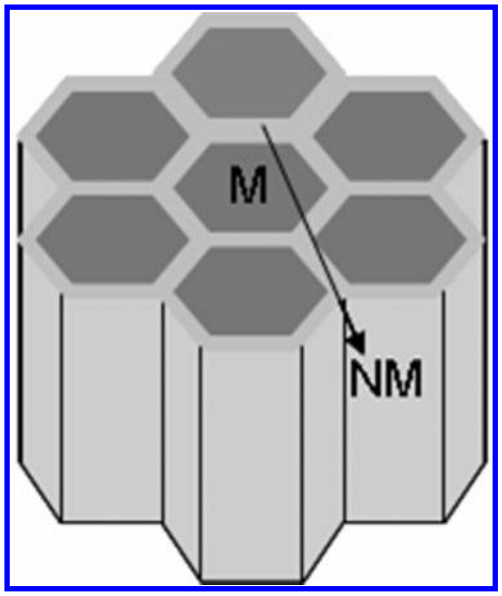

10 Sketch of medium microstructure: magnetic nanograins (M) isolated by non-magnetic boundaries (NM), which is the Cr rich paramagnetic phase for longitudinal media or oxide phase for perpendicular media

5 nm, the exchange field will be doubled. In such a case, the strong exchange coupling is hard to be completely removed by the insufficient non-magnetic phase. This may be another reason why the perpendicular recording media are preferred to the longitudinal ones because the latter needs less exchange coupling to achieve higher SNR.

Chubykalo *et al.*[90] calculated the effect of the exchange coupling on SNR for the longitudinal media. The SNR decreases seriously at the exchange field larger than 1×10^{-6} erg cm^{-1}. In order to achieve higher SNR, it is necessary to downsize grains for a higher areal density, which, however, results in a significant increase in the exchange coupling.[7] On the other hand, our recent results showed that MIPS was obviously suppressed in the downsizing of grains, since the surface/interface energy has a great effect on the MIPS behaviours, owing to its contribution comparable to the chemical free energy. In other words, the longitudinal recording media are in a devil of a hole to decrease the exchange coupling when grains are downsized, and therefore its areal density is limited. The calculation predicts in Fig. 4 that the limited areal density is about 200 Gb in.$^{-2}$ for the Co–Cr–Pt based longitudinal media.

In contrast, the modest exchange coupling in the perpendicular media corresponds to the highest SNR, which has been confirmed by the micromagnetic simulations.[93,94] If the *c* axis orientation could be tilted 45° from the plane normal, the modest exchange coupling would yield another increase of 3–4 dB in the SNR.[93] Nakamura[94] further simulated the contribution of the exchange coupling to the perpendicular media, and found that the somewhat exchange coupling significantly improves SNR at both low and high linear density recording, as shown in Fig. 11, where β_e represents the extent of the intergranular exchange coupling in the Co–Cr perpendicular media. SiO_2 is an effective isolation agent for the perpendicular media, which allows control of the degree of the exchange coupling between the adjacent grains by varying the

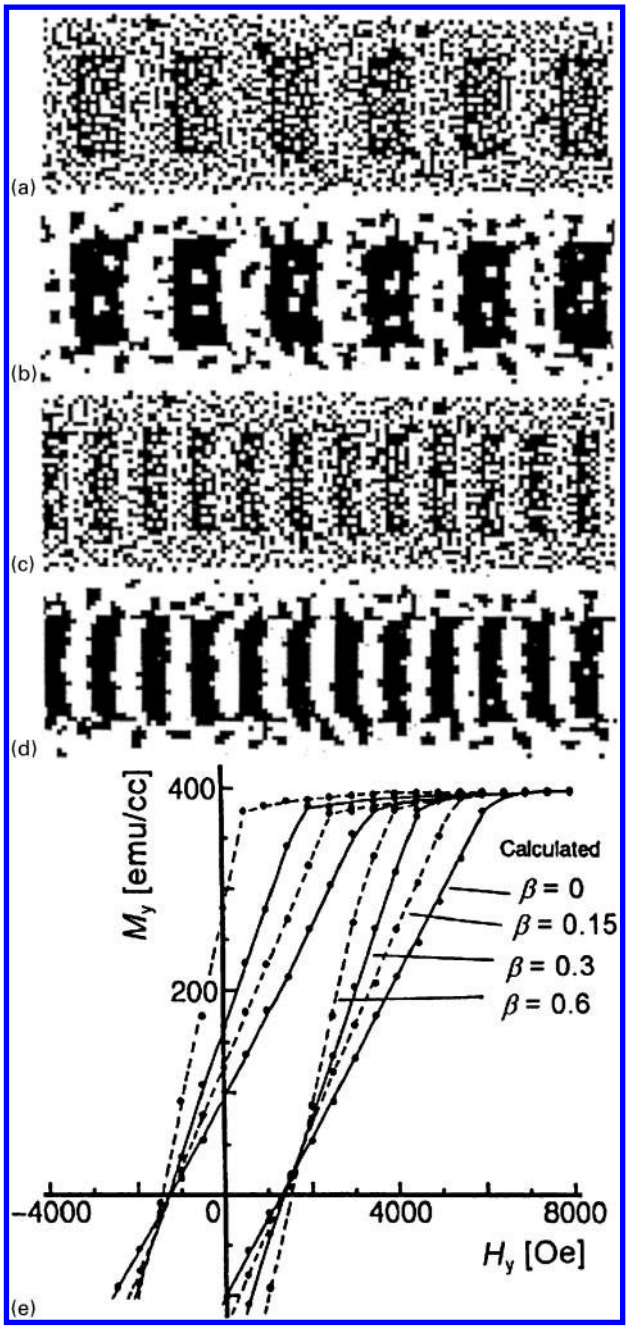

a 100 kFCPI, β_e=0; *b* 100 kFCPI, β_e=0·3; *c* 200 kFCPI, β_e=0; *d* 200 kFCPI, β_e=0·3; *e* magnetic loops with different β_e

11 The micromagnetic simulation[94] on the perpendicular Co–Cr thin film showing the effect of exchange coupling on the magnetisation patterns at bit densities of 100 and 200 kFCPI, and also on magnetic loops (*e*), where β_e represents the extent of the exchange coupling

grain boundary width. However, there have been few reports on how oxide type affects the intergranular exchange coupling. If yes, there will be another possibility to engineer thinner grain boundary to achieve a suitable exchange coupling, and therefore to increase the linear density, especially for the grain sizes less than 10 nm, where the grain boundary width is comparable to grain size. This topic seems, consequently, more important for the future novel media design.

The intergranular exchange coupling has also a significant effect on the transition width *a* of both the

longitudinal and the perpendicular media. Since the linear density is roughly proportional to $1/\pi a$, it becomes an important issue for how to decrease the transition width. Micromagnetic simulation by Peng and Bertram[95] showed the exchange field significantly increases the value of PW_{50} and thus a, in the case of the longitudinal media. But for the perpendicular media, the transition width is the minimal at a modest exchange field of about $0{\cdot}08H_K$, below which both the track width w and the cross-track correlation length s are little affected.[96] When the exchange field is larger than $0{\cdot}1H_K$, all parameters including a, w and s will increase, thus impeding the efforts to increase the areal density.

Texture control

Since the anisotropy axis distribution has a great effect on the magnetic properties of both the longitudinal and perpendicular media, the control of media texture is becoming another important topic.[97–106] For the longitudinal media, micromagnetic calculation [97–100] showed that a low standard deviation of the anisotropy distribution would lead to an increase in coercivity, but to a decrease in the transition noise and the transition width. As a result, a high SNR can be achieved. For example, for a longitudinal medium with a log normal grain distribution and a linear density of 300 kFCPI, the SNR is about 23 dB for a two-dimensional random medium, but about 30 dB for a perfectly textured medium.[98] Generally, the longitudinal media with the in-plane c axis texture are achieved by the epitaxial growth induced by the appropriate underlayers, such as Cr or Cr based alloys, with $(200)_{Cr}//(11{\cdot}0)_{Co}$ or $(112)_{Cr}//(10{\cdot}0)_{Co}$.[100] Actually, this epitaxial growth results in the two-dimensional random distribution of the c axis of grains in the film plane. In order to improve the two-dimensional aligned orientation in the longitudinal media, a circumferentially grooving technique is introduced to create an enhanced orientation ratio along the circumferential direction, and thus to improve the recording properties.[99–101] A slight RF sputtered etching further improves this orientation ratio, which has been ascribed to the ion beam bombardment induced chemical/structural modifications and also to the residual stress in the substrate surface layer.[101] Piramanayagam *et al.* verified that this orientation ratio in the textured media arosed from a thermal effect rather than the previously suggested stress effect.[102]

As compared to the longitudinal media, the orientation ratio is much higher for the perpendicular media due to easy control of the c axis when depositing the Co–Cr–Pt based magnetic layer at room temperature, which yields an improved SNR. Ru intermediate layer, together with a seeding layer, such as Ta, Pd, etc., is usually used to induce c axis of hcp structured Co based recording layer. Since current perpendicular media should have a soft underlayer to facilitate writing, the introduction of Ru intermediate layer between the recording layer and soft underlayer contributes also to decreasing medium noise due to breaking the exchange interaction of them. For the details, please refer to a recent review on this topic by Piramanayagam.[2]

Cheng *et al.* pointed out that the transition width can be further decreased to 40–60%, and therefore, the SNR can be increased by another 3–5 dB if the c axis of media was tilted 45° from the plane normal.[103] Furthermore, the 45° titled media can have a further 62% increase in the areal density and a more rapid switching speed for the media with an anisotropy constant of $K_u = 7 \times 10^6$ erg cm^{-3} as compared to the traditional perpendicular ones.[104] There is little work so far on how to prepare the tilted media. However, two pioneering works imply some promising ways.[105,106] One is to introduce a tilted seedlayer using the oblique physical vapour deposition technique, and then to deposit the desired magnetic layer.[105] By this method, the c axis is tilted, but the grain columns are still perpendicular to the film plane. The other method is to use self-organised and mondispersed nanoparticles as an underlayer, upon which one magnetic layer is deposited. The convex surface of each nanoparticle will make the deposited layer tilted naturally.[106] But the key problems are how to prepare uniform, self-organised nanoparticles on a macroscopic scale and how to decrease the roughness of the film surface, which are indispensable for the ultrahigh density recording.

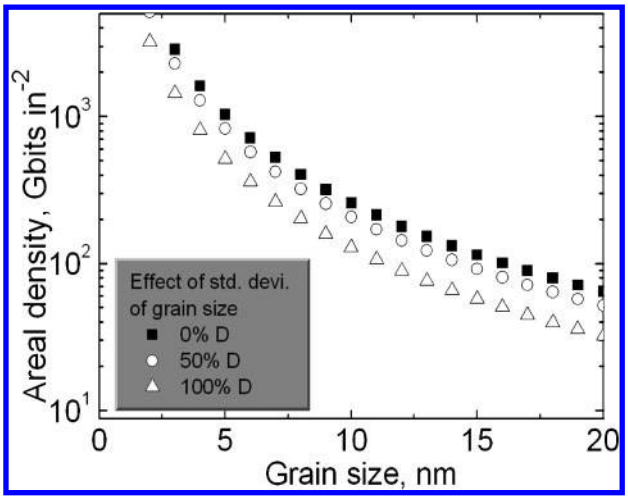

12 Areal density dependence on the grain size and size distribution when the acceptable SNR of 20 dB is set

Grain size engineering

As discussed above, the transition width, jitter, PW_{50}, SNR and thus the areal density are strongly dependent on the in-plane grain size and size distribution. As shown in Fig. 4, the areal density can be increased markedly with decreasing grain size; however, it should be limited by the thermal stability. For instance, for a given medium with an anisotropy constant of 1×10^7 erg cm^{-3} and thickness of 15 nm, the minimal grain size is about 4·6 nm for keeping a good thermal stability, $60k_BT$, at room temperature, which approaches to 1 Tb in.$^{-2}$. If an acceptable SNR of 20 dB for 10 years is assumed, there will be no problem for this medium to reach an areal density of higher than 1 Tb in.$^{-2}$ in the case of the perpendicular recording. Figure 12 illustrates the effect of size distribution on the areal density using equations (9) and (11). If the standard deviation of magnetic grain size changes from 100 to 0%D, the areal density will be doubled. However, when the standard deviation of grain size is less than 50%D, only ~20% gain in the areal density can be attained. Miles[107] simulated the effect of the grain size distribution on the recording properties of the perpendicular media and concluded that a narrow size distribution brings a small jitter and transition width, a high SNR and good thermal stability as well.

For the longitudinal media, if we consider the tradeoff among the magnetic layer composition, anisotropy and exchange coupling, it will not be effective to control the grain size by the intrinsic MIPS through deposition processing, such as temperature, pressure and deposition rate. More useful ways have been proposed through the modification of the epitaxially grown underlayers and/or seedlayers.[108–113] Typically, seedlayers such as NiAl are used to obtain smaller grain size in the case of glass substrates[108] and thin CrX (X=Zr, W, Mo, Ru, Ti, V, etc.) underlayers[109–113] are used in the case of NiP/AlMg substrates. However, it is hard for the NiAl seedlayer to induce the magnetic grain size less than 10 nm and the orientation ratio yet. In contrast, Cr based alloys are the effective underlayers for downsizing magnetic grains.

In 2000, Yoshimura *et al.* utilised the Cr–W seedlayer and the dry etching process to downsize the grains of the Co–Cr–Ta–Ni–Pt medium to $9{\cdot}4\pm2{\cdot}2$ nm.[109] In 2002, Piramanayagam *et al.* further decreased the magnetic grain size of $6{\cdot}2\pm1{\cdot}5$ nm using the Cr–Mo underlayer to $5{\cdot}5\pm2{\cdot}0$ nm using the Cr–W underlayer.[110] W addition is somewhat effective to reduce magnetic grain size but to expand the size distribution, which is not desired for the SNR and yet the transition width. More recently, Sun *et al.* found that doping Ru to the Cr underlayer leads to a remarkable reduction of the grain size of the Co–Cr–Pt–Ta–B media, from $11{\cdot}2\pm2{\cdot}8$ nm for the Cr underlayer to $5{\cdot}4\pm0{\cdot}9$ nm for the Cr–Ru underlayer.[113]

For the hcp structured Co–Cr–Pt based perpendicular media, Ti underlayer can promote the perpendicular orientation. Soo *et al.*[114] found in 2001 that NiP is an effective seedlayer to reduce the grain size of the Co–Cr–Pt alloy medium, decreasing from $20{\cdot}7\pm3{\cdot}1$ to $16{\cdot}7\pm2{\cdot}3$ nm. NiAl is one more effective seedlayer to decrease the magnetic grain sizes to $\sim8{\cdot}2$ nm.[115] In both cases, the media were deposited on heated substrates and thus the exchange decoupling of the magnetic grains were achieved by MIPS. Later, Ariake *et al.* optimised the Co–Cr–Pt–Nb media using the Pt underlayer and carbon seedlayer, resulting in a mean magnetic grain size of $\sim7{\cdot}9$ nm.[116] In 2004, Inaba *et al.* introduced SiO_2 into the Co–Cr–Pt media which obviously suppresses the grain growth during room temperature sputtering.[117] An averaged grain diameter of about 5·4 nm was achieved by the addition of $\sim14{\cdot}4$ at.-%SiO_2. However, the magnetic anisotropy of media is somewhat deteriorated.

More recently, a series of work by Piramanayagama *et al.* showed a perfect control of the grain size of the Co–Cr–Pt based perpendicular media.[118–120] In 2006, their group pointed out the Ru–Cr oxidised intermediate layer induces the Co–Cr–Pt–SiO_2 granular media with an averaged grain size of about $6{\cdot}4\pm0{\cdot}8$ nm. In 2007, they found that the Ru–Cu underlayer further decreased the grain size to ~6 nm,[119] and the utility of an extremely thin synthetic nucleation layer between the intermediate layers Ta and Ru significantly decreased the grain size of the Co–Cr–Pt–SiO_2 medium to $5{\cdot}5\pm0{\cdot}7$ nm, the smallest grain size and size distribution so far.[120]

Future media beyond 1 Tb in.$^{-2}$

Continuing increase in the areal density of the current Co–Cr–Pt based media is limited by the insufficient thermal stability, which is balanced with SNR and writability. The perpendicular recording has exhibited several advantages over the longitudinal recording, as discussed above, which are summarised as follows:

(i) high SNR gain in the perpendicular media for a given thermal stability since they can be designed as 'slim and tall' grains media

(ii) perpendicular head geometry, together with the soft magnetic underlayer, enables a significant boost in the write field strength and also sharper write field gradients at the side and trailing edges, thereby allowing higher anisotropy media and higher track density recording respectively

(iii) several potential technologies, as will be discussed below, to achieve higher density recording, are generally based on the perpendicular recording geometry, which may exploit some feasibility in the future recording integration. Roughly speaking, as also calculated in the section on 'Fundamental magnetism of magnetic recording media', the longitudinal recording may be limited to an areal density of ~200 Gb in.$^{-2}$, whereas the traditional perpendicular recording can reach 500 Gb in.$^{-2}$, although very hard beyond 1 Tb in.$^{-2}$.

In order to increase the areal density approaching 1 Tb in.$^{-2}$ and above, several proposals have been addressed so far to try to solve the 'trilemma' problems. These include percolated perpendicular media,[121–128] bit patterned media,[129–152] heat assisted media,[153–164] continuous granular composite media (CGC)[165–169] and exchange spring media.[170–175] Since last two kinds of media (CGC media and exchange spring media) have been well documented in the literature,[165–175] we focus our attention in this section only on the first three cases, in particular, with respect to their principles of magnetism, media development from a viewpoint of materials science, engineering progress so far and directions in the near future.

Percolated perpendicular media

Granular perpendicular media (GPM), usually Co–Cr–Pt based oxide composite, are the currently leading media for commercial perpendicular hard disk memories. In order to achieve a high SNR and thus the areal density, the grain size and size distribution should be decreased to minimise the transition noise while maintaining the sufficient thermal stability, which is completely in the dilemma, as discussed above. One novel idea has been firstly proposed by Zhu *et al.* in 2006,[121–122] and then modelled by Suess *et al.*,[123] to introduce a second nanophase to the magnetic layer as pinning sites, and consequently the domain walls of each bit are pinned. A sharper transition boundary is thus expected if the size and distribution of the second nanophase are controlled reasonably, as schematically shown in Fig. 13. In such a way, it becomes possible for independent control of the SNR and thermal stability. In other words, the dilemma above can be solved. This kind of media is named as the percolated perpendicular media (PPM), which might be better understood by the name of 'magnetic domain wall recording media'. It is believed to reach an areal density approaching 1 Tb in.$^{-2}$ and beyond.

The magnetisation of the conventional GPM is governed by the magnetic rotation mechanism while that of PPM is governed by the nucleation and domain

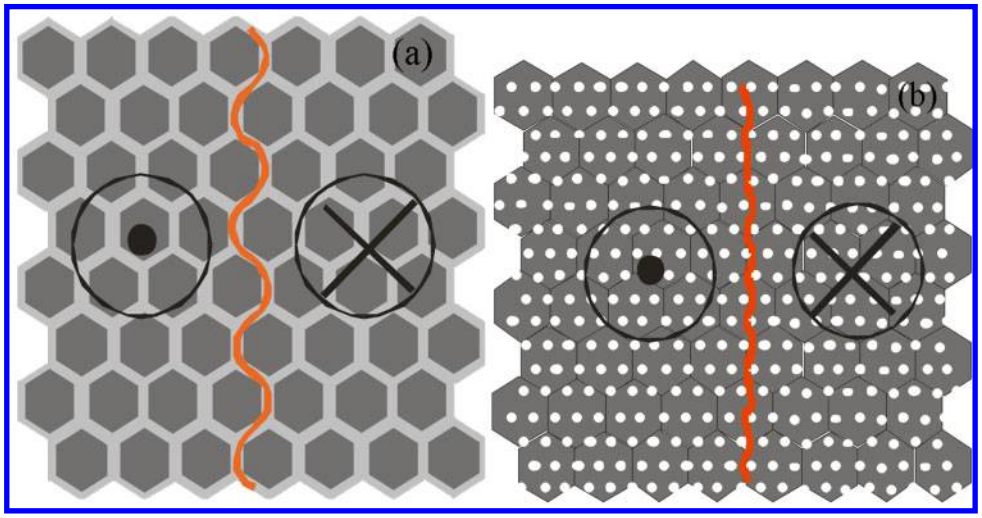

13 Sketches of *a* traditional granular perpendicular media and *b* percolated perpendicular media: the transition parameter mainly depends on the grain size and exchanging coupling in *a*, while it mainly depends on the density, size and regular distribution of the pinning sites in *b*, where the white spots represent the pinning nanophase

wall motion and pinning. Therefore, they have shown a big difference, not only in the transition noise, but also in the thermal stability, switching time and so on.[121–123]

The switching time, which is known to be a key technical parameter of the media, depends strongly on the damping constant α_d for GPM. For example, the switching time changes from $\sim$5 ns for α_d=0·01 to $\sim$0·5 ns for α_d=0·1. In contrast, the switching time varies slightly with α_d for the PPM and generally is below 1 ns.[122] The dependence of the switching field on the switching time is similar, too.[122] Both of them are due to the difference in the magnetisation reversal mechanism.

When one considers the Bloch domain wall energy, $4S(AK_1)^{1/2}$, and magnetic rotation energy K_1V, where S is the in-plane grain area and V is the grain volume, the film thickness should be larger than a critical value, $4(AK_1{}^{-1})^{1/2}$ as documented in equation (3), which is energetically favourable for domain wall motion. Otherwise, the magnetic rotation reversal is energetically favourable. The wall thickness is usually expressed by $\pi(AK_1{}^{-1})^{1/2}$. The micromagnetic simulation showed that the pinning nanophases play a role only when they have a size comparable to the wall thickness. The pinning field depends on the diameter and density of the pinning nanophases.[121–123]

The detailed simulations have been addressed by Zhu and Tang,[121] Tang and Zhu[122] and Suees *et al.*[123], and some important conclusions have been made, which could guide future design of the PPM. First of all, the coercivity of the PPM is roughly proportional to the area density of the pinning nanophase, especially for a pinning size comparable to the domain wall thickness. For example, the coercivity increases from about 0·4H_K without any pinning nanophase to about 0·8H_K with 50% nanophase included for a medium with an anisotropy constant of 1×10^7 erg cm^{-3}, a saturation magnetisation of 1000 emu cm^{-3} and a normalised exchange coupling constant of 0·4.[121] However, the exchange coupling constant slightly decreases the coercivity and saturates the coercivity to about 0·5H_K when the normalised exchange coupling constant is larger than 0·2.[122]

The exchange coupling has also a great effect on the media noise. Without any exchange coupling, PPM has a large switching field distribution. Accordingly, the medium noise is dominated by the DC noise. But the medium noise is rapidly decreased by the exchange coupling because of the pinning effect and smaller switching field distribution. A larger exchange coupling will increase the media noise again due to the ineffective pinning.[122] Zhu and Tang[124] further elucidated the pinning effect, and they concluded that the pinning nanophase size of about (½–1)$\pi(AK_1{}^{-1})^{1/2}$ corresponds to the lowest medium noise, whereas the nanophase size of (2/5–⅔)$\pi(AK_1{}^{-1})^{1/2}$ corresponds to the largest thermal stability ($\sim$45K_BT at T=333 K). The transition parameter and jitter are much smaller in the PPM than in the GPM, and regularly arrayed pinning nanophases will further reduce them to less than 0·5 nm, even several times less than that in the GPM.[121]

In the micromagnetic simulations,[121–123] the exchange stiffness is considered as a constant. However, it is actually a variable which depends strongly on the grain size.[7] For this reason, the theoretical calculations may deviate from the experimental results. Furthermore, the grain size of the magnetic layer will be a useful engineering parameter to design the proper exchange coupling strength for a given medium material.

Laughlin *et al.* firstly[125,126] attempted to prepare the PPM in 2007 by annealing the traditional hcp structured Co–Pt–SiO_2 GPM. They found that the pinning effect will become significant if the volume of SiO_2 and annealing process are well controlled to obtain the SiO_2 nanopillars instead of the SiO_2 nanospheres. The maximum coercivity of $\sim$4 kOe was achieved in the Co–16Pt PPM annealed at 600–650°C for 1–5 min. Choice of any other temperature range and time duration or of a higher SiO_2 volume will lead to poor magnetic properties. However, the work by Sun *et al.*[127] showed that the precipitation of MgO nanodots in the FePt matrix contributes to an increased the medium coercivity, which is quite different from the statement by Laughlin *et al.*[125,126] that only the oxide nanopillars are effective for pinning. Consequently, more work should be conducted in the near future to understand the

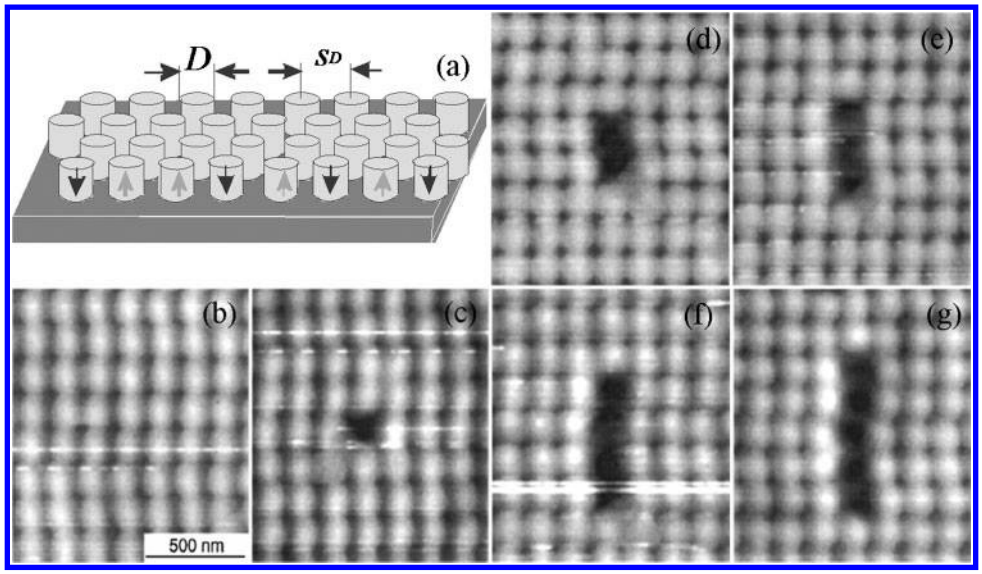

14 Bit patterned medium: *a* sketch of BPM and *b–g* showing the *in situ* MFM images[140] during the process of writing 5 bits on a 29 Gdots in.$^{-2}$ medium (Co–Cr–Pt film) with a perpendicular anisotropy: *b* initial DC erased states and *c–g* corresponding to 1–5 written bits in the downward direction

pinning effects, e.g. the effects of oxide volume, distribution, shape and categories as well as magnetic layer features such as structure, composition and thickness, and optimised annealing process.

Rahman *et al.*[128] recently proposed another kind of PPM, Co/Pt multilayer on one nanoporous anodised alumina. The magnetic domain walls are pinned by the nanopores rather than by the aforementioned second phases. The coercivity of the PPM is proportional to the pore density, but the switching field is insensitive to the angular deviation of $\sim 50^{\circ}$ from the easy axis. It suggests that the nanopores pinned PPM provides large tolerance for the switching field distribution, and may be one solution for the problem of adjacent track erasure.[128] Even so, the nanopore pinned PPM for future 1 Tb in.$^{-2}$ should have a smaller pore size of ~ 4 nm and a regular pore distance of ~ 5 nm. However, it is hard to achieve this kind of microstructure for the state of the art anodic oxidisation technique, and any novel processing is absolutely necessary in the near future.

Bit patterned media

The idea of the patterned media was proposed by Chou and Krauss[129] and developed by White *et al.*,[130] aiming at postponing the onset of the spuerparamagnetism problem of recording media, where the energy barrier KV is increased by replacing the grain volume V with the switching volume of each bit (or island) for a given anisotropy (K) medium. In this case, the grains inside one bit are highly exchange coupled and behave like a single domain, rather than like that in traditional longitudinal media which requires decoupling of the grains so that the magnetisation reversal of each grain is proceeded by magnetic rotation. Chappert *et al.*[131] then suggested a feasible way to prepare this kind of media by ion irradiation through a lithographically patterned resist mask. In general, the patterned media includes track patterned media[132] and BPM,[133] as schematically shown in Fig. 14*a*. The latter shows a higher density approaching to several Tb in.$^{-2}$ and is accordingly paid much attention in recent years.[134,135] In the initial bit patterned media, White *et al.*[130] suggested a ring head, in which the easy axis of each bit, lying in the film plane, parallels to the applied field. For a polycrystalline Co–Cr–Pt based alloy layer, it is impossible to produce this kind of high orientation by sputtering. Even if single crystal MgO substrate was used to align the texture of media later,[136] the progress was limited due to the intrinsic structure feature of the hcp cobalt alloys. An alternative approach is to orient the easy axis normal to the film plane, i.e. bits are patterned in the perpendicular media by the lithography. In such a processing, it is generally easy to control the texture of the hcp structured Co based media with the help of proper seedlayers and underlayers.[53–55]

The major magnetism requirements of the BPM have been summarised by Terris and Thomson[134] as follows:

(i) each bit (or island) must be of a single domain remanent state, and also the medium has a well defined uniaxial easy axis to keep the easy axis of the bit a constant orientation in relation to the head read/write elements

(ii) the coercivity and anisotropy need to match the available writing field

(iii) the switching field distribution (SFD) must be sufficiently narrow so that the writing head field gradient addresses only the island intended to be written

(iv) the islands must be thermally stable with the appropriate saturation magnetisation, and should also be available for the optimisation of recording, thermal stability and readback signal amplitude.

From which one can find that these requirements are quite similar as the conventional perpendicular media, except for being the predefined bit location. When the head flies over the islands during recording, the writing field pulse should be in harmony with the exact bit positions, and any deviation will lead to a written-in error. Accordingly, the written-in error may arise from all the standard deviations of media parameters, such as the switching field distribution, the magnetostatic interaction, the bit spacing deviation in one two-dimensional film plane, the bit diameter and so on.

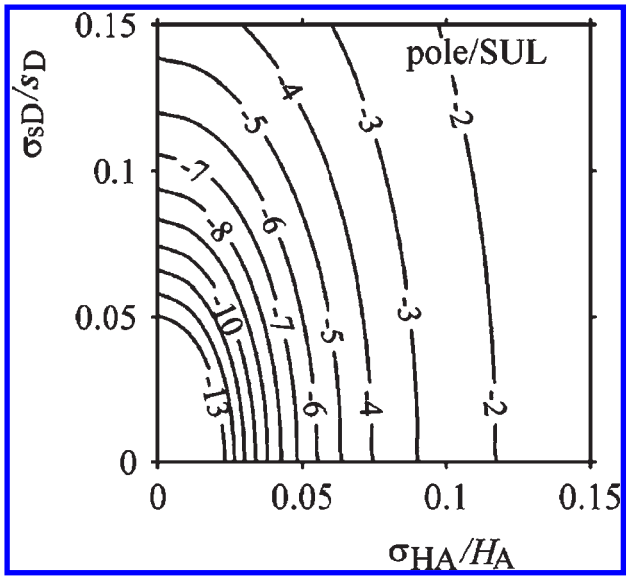

15 Contour plots of BER (in decades) for the effect of distribution of the anisotropy fields and bit positions for a pole head/SUL combination at a density of 1 Tb in.$^{-2}$ (Ref. 135)

For the detailed analysis, please refer to the literature by Richter *et al.*[135] Richter *et al.* calculated the contour plots of the bit error rate (BER) for the effect of distribution of the anisotropy fields and bit positions. An example is given here for a pole head/SUL combination at a density of 1 Tb in.$^{-2}$,[135] as shown in Fig. 15. A narrow distribution of both the anisotropy and the bit position decreases the BER remarkably and thus provides a high SNR^{BPM}.

Considering the noise sources of the bit spacing fluctuation and bit size fluctuation, Richter *et al.* wrote the SNR^{BPM} as follows[135]

$$SNR^{BPM} \approx \frac{1}{2\cdot 4(\sigma_{s_D}/s_D)^2 + 4(\sigma_D/D)^2} \quad (16)$$

where s_D and D are the bit spacing and diameter respectively, and σ_{s_D} and σ_D are their standard deviations. Of course, the effects of the saturation magnetisation fluctuation and bit thickness fluctuation on the SNR^{BPM} can be simply added into equation (16) as the additional terms in the denominator.

The engineering of the BPM has been performed by many groups up to date,[137–139] but is still a challenging topic, especially for the 10–20 nm bit size. Generally, the bit patterns are generated by the lithography method,[137] phase separated copolymers[138] or alumina anodic oxidisation (AAO)[139] to predefine a regular template, and then the bits are formed either by the following electrodeposition or sputtering, called additive patterning process, or by etching or ion milling to regularly removed unwanted parts to get bits separation, called subtractive patterning process.[134]

In 1999, Haginoya *et al.*[140] presented a BPM demonstration of 29 Gb in.$^{-2}$, with the bit diameter of 80 nm and height of 40 nm, as shown in Fig. 14*b–g*. The Co–Cr–Pt perpendicular medium was firstly prepared by sputtering and then patterned by electron beam lithography to get this BPM, and the bits were recorded by the current flowing assisted heating between the MFM tip and the bits. Figure 14*c–g* showed that 1–5 bits were recorded in sequence.

The progress of the BPM[129–140] shows some potentials for the future high density recording, but there are yet some challenges toward 1 Tb in.$^{-2}$ and beyond. First, for the areal density of ~1 Tb in.$^{-2}$, the bit size should be around 10–20 nm in diameter. Considering the limit of wavelength of the used electromagnetic waves, such as extremely UV, X-ray and electron beam, it is very hard to pattern bits below sub-20 nm for the time being. Electron beam lithography is possible, but suffers from low efficiency and high cost.[137] This is also the case for the AAO template, by which it is very hard to tune smaller bit spacing for a bit size of less than 20 nm.[139] Second, the Tb in.$^{-2}$ density recording requires a head to media spacing of sub-10 nm, usually ~5 nm. If any resist residue or contamination due to incomplete cleaning during the patterning process is left on bits surface, it will cause fatal damage to a magnetic head. Third, bit patterning manufacture, as described above, is a multistep process and thus cost ineffective as compared to the conventional sputtered media. Since the processing cost is a big obstacle, any promising manufacture methods that can simplify the patterning process are expected to bring a bright prospect for the BPM.

An alternative promising technology is the self-organisation of magnetic nanoparticles.[141] The essential of this approach is to chemically prepare high anisotropy magnetic nanoparticles, such as FePt and CoPt, through polyol or modified polyol method to reduce metal ions to form the desired nanoparticles, and the nanoparticle size is usually controlled using suitable capping agents (or surfactants) and by adjusting reaction temperatures during the synthesis process, finally selected by the size selection method such as centrifuging. With such a method, a perfect and narrow size distribution can be obtained as small as 5%. The BPM is generally formed by the self-organisation of these nanoparticles since their surfaces are capped by one layer surfactants, which are cross-linked leading to the uniform separation of these nanoparticles. In this case, the separation of the magnetic nanoparticles is controlled by the balance among magnetic dipolar interaction, van der Waal's force, electrostatic interaction, and the features of surfactants such as size and molecular weight when they are deposited on one substrate.

Sun *et al.*[141] first demonstrated two-dimensional film of monodisperse and self-organised FePt nanoparticles with a tunable size 4–10 nm and very narrow size distribution of ~5%, and thus suggested it be one promising medium for future high density recording. However, many challenges have to be overcome before the FePt nanoparticles can be used as recording media. First, the chemically prepared FePt nanoparticles are usually of fcc structure with very low anisotropy. A post-annealing process can cause ordering from fcc to fct structure which owns a high magnetic anisotropy, but causes the coarsening of the particles and an undesired broad size distribution. The alloying method has been tuned out to be effective in decreasing ordering temperatures of the FePt nanoparticles if Cu,[142] Ag,[143] Au[144] and Sb[145] are reduced together with Fe and Pt ions to form the ternary Fe–Pt–X (X=Ag, Au, Cu)

nanoparticles. In 2006, Nguyen *et al.*[146] proposed one promising synthesis method, in which $Na_2Fe(CO)_4$ and $Pt(acac)_2$ were used as reagents to directly get ordered FePt nanoparticles in one step without any post-annealing. Rong *et al.*[147] presented the so called 'salt-matrix annealing' technique to order FePt nanoparticles, by which the growth of the particles during the annealing is suppressed effectively. Wiedwald *et al.*[148] found that He^+ ion irradiation can lower $L1_0$ ordering temperature of the FePt nanoparticles in 2007.

The second challenge to the media application of FePt nanoparticles is how to obtain a perfect texture, namely, how to orient their easy axes of each nanoparticle in the direction perpendicular to the film plane. Actually, it is very hard, if not impossible, since the orientation distribution is random in three dimensions. Harrell *et al.*[149] tried to illustrate the feasibility of aligning the easy axis of the $L1_0$ FePt nanoparticles. Their calculation showed that the two factors govern the orientation, the degree of alignment of the magnetic moment and the coupling between the easy axis and the magnetic moment. However, the prediction by calculation was imperfect with respect to the experiments of the arrangement of the FePt nanoparticles. They claimed that many other factors could also contribute to the alignment of the easy axis of nanoparticles, such as the distribution in the particle size and particle anisotropy, the interparticle interaction and clustering during drying. Even so, the work by Qiu *et al.*[150] showed that the external magnetic field can align the easy axis orientation of the ordered FePt nanoparticles in plane or out of plane more or less, but not perfectly.

The third challenge to the FePt nanoparticles is how to self-organise themselves on a macroscopic scale, e.g. on a centimeter scale from one point of view of application. The perfect image of regularly aligned FePt nanoparticles, such as in TEM observation,[141] is only limited to a micrometer scale. The self-organisation of the nanoparticles becomes not uniform on a larger scale and some areas are usually absent of any nanoparticles. Kodama *et al.*[151] proposed a special spin coating technique to enable a dense array of the FePt nanoparticles across the entire surface of a 2·5 in. disk substrate, but with a random orientation.

A more recent pioneering work by Kim *et al.*[152] may push the use of the FePt nanoparticles as a real recording medium. The FePt nanoparticles with a perfect perpendicular easy axis, small size ($\sim$18 nm), large out-of-plane coercivity $\sim$15 kOe and extremely high density $\sim$1 Tb in.$^{-2}$ were achieved using the AAO template technique followed by a rapid annealing.

Heat assisted recording

To keep sufficient KV against $60k_BT$ for the thermal stability and high SNR at an increased areal density, media with high K are needed while suffer from the head writability problem. Even though the perpendicular recording geometry determines a higher writing field than that of the longitudinal recording, improved by more than 50%, as shown in Fig. 3, the writing field at ambient temperature is not strong enough for high H_C media since $H_C \sim H_K \sim K$ for the general granular media when assuming $\sim$1 Tb in.$^{-2}$ recording (about 25 × 25 nm for 1 bit) and attainably accepted SNR. As a result, a promising approach, HAMR, is proposed to break this dilemma.[153–164]

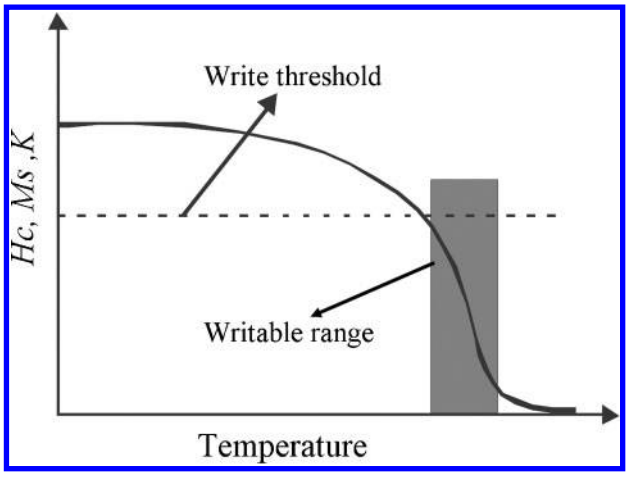

16 Sketch of H_C, M_S and K of medium dependent on temperatures, suggesting available temperature range for writing in the HAMR medium shown in hatched area

The merit of HAMR is rested with localised heating of the medium during the writing process, followed by a rapid cooling back to ambient temperature. High K at ambient temperature is needed to retain the thermal stability but the writability is overcome by heating the medium during recording, as shown schematically in Fig. 16. The temperature dependent magnetic anisotropy K and H_C of one medium are reduced because of the negative slope as the medium is warmed toward its Curie temperature. The H_C is reduced well below the write threshold of the head. In principle, the HAMR is one kind of thermomagnetic recording, in analogy with the mature technology, magnetic–optical recording (MO), developed in the 1980s.[155,156] The difference rests with its extreme reduction of spatial and temporal scale and the introduction into the HDD architecture.[153]

As revealed by the essence of HAMR, its areal density is determined by the size of spot and light transmission efficiency, i.e. effectively heating in a small location, which is also in the dilemma.[153] First, the spot size d_{ss} is given by[153]

$$d_{ss} = \frac{0{\cdot}51\lambda}{n \sin \theta_L} \tag{17}$$

where λ is the wavelength of the incident light, n is the refractive index of media and θ_L is a half of the angle of the marginal light. Actually d_{ss} is limited by the diffraction of the incident light, always over than $\sim$200 nm for the visible light. Several approaches have been addressed to minimize the d_{ss} value. Solid immersion lenses, proposed by Mansfield and Kino,[157] provide a higher numerical aperture by n^2 times ($\sim$2); therefore, the spot size of sub-100 nm becomes possible.[17,153] However, it is still hard to get a spot size of less than 50 nm since there are no materials with a refraction index as high as 4.[153] Of course, the spot size can be alternatively decreased by controlling the aperture size. However, the transmission energy of the light becomes so low that a local and high heating efficiency cannot be ensured.[158] Suzuki *et al.*[159] showed the linear decrease in the focusing depth, namely, the allowed recording layer thickness, with the spot size. The maximum magnetic layer thickness should be less than 20 nm for a spot size under 100 nm. Thereby, the dilemma problem occurs when the spot is downsized. Solid immersion lens can

provide effective heating, but the spot size is large. The aperture can determine arbitrarily small spots, but the effective heat energy is low.

Fortunately, the recent work by McDaniel *et al.*[153,160–162] showed that the surface plasma effect can enhance the heat transmission through the sub-100 nm holes, provided that Au or Ag thin films were used. A more recent work by Ng *et al.* in 2007[163] found that media can be heated by the field emission and a moderate ionisation generated between the head tip and medium surface, indicating another way to achieve much smaller heating area.

The other difference between the HAMR and conventional recording is in the writing field gradient dH/dx. The areal density and SNR are closely related to the transition parameter a, which is a function of $1/(dH/dx)$. Therefore, the larger the dH/dx, the higher the areal density can reach. For the conventional recording, the effective write field gradient $(dH/dx)_{eff}$ is determined simply by the write head. For HAMR, it can be expressed as follows[153]

$$\left(\frac{dH}{dx}\right)_{eff} \approx -\frac{dH_C}{dT}\frac{dT}{dx} \tag{18}$$

where dH_C/dT is the medium coercivity dependence of temperatures, and dT/dx is the spatial gradient of temperature in the medium heated by the local incident light. This effective field gradient is much stronger than that for the conventional magnetic heads. It can thus be expected that the media with a high coercivity–temperature coefficient and subjected to a confined heating on a nanometre scale enable a high areal density. In other words, the HAMR has another gain in SNR, and thus, a higher areal density than that of the conventional recording at ambient temperature.

Even so, HAMR has encountered several engineering challenges. One is the highly integrated magnetic head with the effective and small components of both magnetic and optical ones. The second one is how to improve the heat efficiency. Since only several percentages of heat generated by the heat source are used to increase medium temperatures,[153] much of the heat is wasted and may deteriorate the head, and do harm even to SNR.[164] The third is how to effectively hinder the temperature rise of the magnetic head due to the dissipated heat. Attention should be paid to the specific suspension with high heat conductivity and sink, together with air bearing in the future development of HAMR. The fourth is the thermal stress effect, which has been overlooked so far. It is supposed that the thermal stress generated by very large temperature gradients may make film surface curved (convex and concave) on a nanometre scale, and even minor cracking with a recording history of thousands of times and more. In the latter case, the writing and reading of the HAMR media will fail.

Summary and outlook

The longitudinal recording media based on the Co–Cr–Pt based alloys as magnetic recording layers have reached a limit of the areal density of 100–200 Gb in.$^{-2}$ due to a broad distribution of the anisotropy, magnetisation and orientation of easy axis arising from the intrinsic phase separation during the sputtering process, which results in the exchange decoupling of magnetic grains but a chemical inhomogeneity both in grain interiors and along grain boundaries. In contrast, the perpendicular recording provides higher writability and achievable SNR through the grain aspect design, the tunable exchange coupling, and also the narrow distribution in composition, grain size and anisotropy derived from the oxide isolated granular media as well as the perfect orientation of the easy axis. With proper tailoring of the grain size, the texture and the intergranular exchange coupling, the areal density for the perpendicular media can be $\sim$500 Gb in.$^{-2}$ and beyond. For the much higher density recording towards Tb in.$^{-2}$, the conventional perpendicular recording is hard to achieve this objective. However, a combination with the other techniques would be feasible in the near future, such as BPM with HAMR, composite media with HAMR, percolated perpendicular media with HAMR.

Acknowledgements

The authors sincerely appreciate Professor O. Kitakami and Professor Y. Shimada, Institute of Multidisciplinary Research for Advanced Materials, Tohoku University, Japan, and Professor J. R. Gao, Key Lab of EPM, Northeastern University, China, for their critical review on this manuscript and highly valuable suggestions on the final manuscript improvement. The authors should thank two reviewers for their thoughtful suggestions to improve the manuscript, and should appreciate also the following organisations for permission to reproduce the following figures: American Institute of Physics, New York, USA (Figs. 9*c–d* and 14); Elsevier Science BV, Amsterdam, The Netherlands (Figs. 8, 9*a* and 11); the Magnetic Society of Japan, Tokyo, Japan (Fig. 9*b*); Institute of Electrical Electronics and Engineers Inc. (IEEE), Piscataway, NJ, USA (Fig. 15). The work was supported by the National Natural Science Foundation of China (no. 50671020) and Chinese Ministry of Education (no. 108039).

References

1. Y. Nakamura: *Magune*, 2006, **1**, (5), 190–196.
2. S. N. Piramanayagam: *J. Appl. Phys.*, 2007, **102**, 011301–011322.
3. Available at: http://www.physorg.com/news136815757.html
4. H. Coufal, L. Dhar and C. D. Mee: *MRS Bull.*, 2006, **31**, 374–378.
5. S. Parkin: *MRS Bull.*, 2006, **31**, 389–394; S. Khizroev and D. Litvinov: *J. Appl. Phys.*, 2004, **95**, (9), 4521–4537.
6. S. N. Mao, L. Wang, C. H. Hou and K. Murdock: *IEEE Trans. Magn.*, 2003, **39**, (5), 2396–2398; Y. Kanai, R. Matsubara, H. Watanabe and Y. Nakamura: *IEEE Trans. Magn.*, 2003, **39**, (4), 1955–1960; K. Gao and H. N. Bertram: *IEEE Trans. Magn.*, 2003, **39**, (2), 704–709.
7. H. J. Richter: *J. Phys. D*, 1999, **32D**, 147–168; *J. Phys. D*, 2007, **40D**, 149–177.
8. M. H. Kryder, W. Messner and L. R. Carley: *J. Appl. Phys.*, 1996, **79**, (8), 4485–4490.
9. D. Weller and A. Moser: *IEEE Trans. Magn.*, 1999, **35**, (6), 4423–4439.
10. Z. Y. Zhang and G. Tarnopolsky: *IEEE Trans. Magn.*, 2001, **37**, (4), 1260–1263.
11. D. Weller and M. F. Doerner: *Annu. Rev. Mater. Sci.*, 2000, **30**, 611–644.
12. R. W. Wood, J. Miles and T. Olson: *IEEE Trans. Magn.*, 2002, **38**, (4), 1711–1718.
13. R. H. Victora, J. H. Xue and M. Patwari: *IEEE Trans. Magn.*, 2002, **38**, (5), 1886–1889.
14. N. Honda, K. Yamakawa and K. Ouchi: *IEEE Trans. Magn.*, 2007, **43**, (6), 2142–2144.

15. H. N. Bertram, H. Zhou and R. Gustafson: *IEEE Trans. Magn.*, 1998, **34**, (4), 1845–1847.
16. H. N. Bertram and M. Williams: *IEEE Trans. Magn.*, 2000, **36**, (1), 4–9.
17. R. L. Comstock: 'Introduction to magnetism and magnetic recording', 297, 439; 1999, New York, John Willey & Sons.
18. X. W. Wu, R. J. M. van de Veerdonk, B. Lu and D. Weller: *J. Magn. Magn. Mater.*, 2006, **303**, 261–264.
19. X. Z. Cheng and M. B. A. Jalil: *IEEE Trans. Magn.*, 2005, **41**, (10), 3115–3117.
20. H. N. Bertram: 'Theory of magnetic recording', 261; 1994, Cambridge, Cambridge University Press.
21. H. Zhou and H. N. Bertram: *IEEE Trans. Magn.*, 2000, **36**, (1), 61–66.
22. B. K. Middleton and J. J. Miles: *IEEE Trans. Magn.*, 2001, **37**, (4), 1327–1329.
23. H. N. Bertram and H. J. Richter: *J. Appl. Phys.*, 1999, **85**, (8), 4991–4998.
24. N. Kikuchi, O. Kitakami, S. Okamoto and Y. Shimada: *J. Phys., Condens. Matter*, 1999, **11**, (43), 485–490.
25. O. Kitakami, N. Kikuchi, S. Okamoto and Y. Shimada: *J. Magn. Magn. Mater.*, 1999, **202**, (2–3), 305–310.
26. M. Hasebe, K. Oikawa and T. Nishizawa: *J. Jpn Inst. Met.*, 1982, **46**, 577–583.
27. Y. Maeda, S. Hirono and M. Asahi: *Jpn J. Appl. Phys.*, 1985, **24**, L951–L953.
28. G. W. Qin, K. Oikawa, T. Ikeshoji and K. Ishida: *J. Magn. Magn. Mater.*, 2001, **234**, (1), 1–4.
29. H. Kaneko, M. Homma and K. Nakamura: *AIP Conf. Proc.*, 1971, **5**, 1088–1092.
30. T. Nishizawa, M. Ko and M. Hasebe: *Acta Metall.*, 1979, **27**, 817–828.
31. C. Allibert, C. Bernard, N. Valignat and M. Dombre: *J. Less-Common Met.*, 1978, **59**, 211–216.
32. J. C. Lin, and Y. A. Chang: *Metall. Mater. Trans. A*, 1988, **19A**, (3), 441–446.
33. K. Oikawa, G. W. Qin, O. Kitakami and K. Ishida: *Appl. Phys. Lett.*, 2001, **79**, 644–646.
34. K. Oikawa, G. W. Qin, T. Ikeshoji and K. Ishida: *J. Magn. Magn. Mater.*, 2001, **236**, (1–2), 220–233.
35. K. Oikawa, G. W. Qin, S. Okamoto, K. Ishida and Y. Shimada: *Appl. Phys. Lett.*, 2002, **80**, (15), 2704–2706.
36. M. Hillert and M. Jarl: *Calphad*, 1978, **2**, 227–238.
37. Y. Ikeda, Y. Sonobe, H. Uchida and T. Toyooka: *IEEE Trans. Magn.*, 1997, **33**, (5), 3079–3081.
38. O. Kitakami, N. Kikuchi, S. Okamoto and Y. Shimada: *J. Magn. Magn. Mater.*, 1999, **202**, 305–310.
39. N. Inaba, T. Yamamoto and Y. Hosoe: *J. Magn. Magn. Mater.*, 1997, **168**, 222–231.
40. K. Oikawa, G. W. Qin, O. Kitakami, Y. Shimada, K. Ishida and K. Fukamichi: *J. Magn. Soc. Jpn*, 2001, **25**, 478–485.
41. Y. Hirayama, M. Futamoto and K. Kimoto: *IEEE Trans. Magn.*, 1996, **32**, 3807–3809.
42. Y. Kubota, L. Folks and E. E. Marinero: *J. Appl. Phys.*, 1998, **84**, 6202–6204.
43. C. R. Park, I. Suzuki, N. Tani, Y. Ota and K. Nakamura: *IEEE Trans. Magn.*, 1992, **28**, 3084–3086.
44. M. Doener, X. Bian, M. Madison and M. Pinarbasi: *IEEE Trans. Magn.*, 2001, **37**, 1502–1504.
45. R. L. Comstock: *J. Mater. Sci., Mater. Electron.*, 2002, **13**, 509–523.
46. E. N. Abarra, A. Inomata, H. Sato, I. Okamoto and Y. Mizoshita: *Appl. Phys. Lett.*, 2000, **77**, (6), 2581–2583;
47. E. E. Fullerton, D. T. Margulies, M. E. Schabes, M. Carey, B. Gurney, A. Moser, M. Best, G. Zeltzer, K. Rubin, H. Rosen and M. Doerner: *Appl. Phys. Lett.*, 2000, **77**, (23), 3806–3808.
48. I. R. McFadyen, E. E. Fullerton and M. J. Carey: *MRS Bull.*, 2006, **31**, (5), 379–383.
49. S. Iwasaki and Y. Nakamura: *IEEE Trans. Magn.*, 1977, **13**, (5), 1272–1277.
50. H. N. Bertram and V. L. Safonov: *Appl. Phys. Lett.*, 2001, **79**, (26), 4402–4404.
51. Q. Peng and H. J. Richter: *J. Appl. Phys.*, 2003, **93**, (10), 7399–7381.
52. O. Kitakami, T. Shimatsu, S. Okamoto, Y. Shimada and H. Aoi: *Jpn J. Appl. Phys.*, 2004, **43**, (1A/B), 115–117.
53. T. Shimatsu, H. Sato, T. Oikawa, Y. Inaba, O. Kitakami, S. Okamoto, H. Aoi and Y. Nakamura: *IEEE Trans. Magn.*, 2005, **41**, (2), 566–571.
54. T. Shimatsu, H. Sato, K. Mitsuzuka, T. Oikawa, Y. Inaba, H. Aoi, H. Muraoka, Y. Nakamura, O. Kitakami and S. Okamoto: *J. Appl. Phys.*, 2005, **97**, 10N1111-1-3.
55. H. Sato, T. Shimatsu, Y. Okazaki, O. Kitakami, S. Okamoto, H. Aoi, H. Muraoka and Y. Nakamura: *IEEE Trans. Magn.*, 2007, **43**, (6), 2106–2108.
56. D. Suess, T. Schrefl, S. Fahler, M. Krschner, G. Hrkac, F. Dorfbauer and J. Fidler: *Appl. Phys. Lett.*, 2005, **87**, 012504–012506.
57. R. H. Victora and X. Shen: *IEEE Trans. Magn.*, 2005, **41**, 537–542.
58. H. J. Richter and A. Dobin: *J. Appl. Phys.*, 2006, **99**, 08Q905–08Q907.
59. A. Y. Dobin and H. J. Richter: *Appl. Phys. Lett.*, 2006, **89**, 062512–062514.
60. T. Shimatsu, Y. Okazaki, H. Sato, O. Kitakami, S. Okamoto, H. Aoi, H. Muraoka and Y. Nakamura: *IEEE Trans. Magn.*, 2007, **43**, (6), 2995–2997.
61. T. Oikawa, M. Nakamura, H. Uwazumi, T. Shimatsu, H. Muraoka and Y. Nakamura: *IEEE Trans. Magn.*, 2002, **38**, (5), 1976–1978.
62. K. Oikawa, G. W. Qin, S. Okamoto, O. Kitakami and K. Ishida: *Appl. Phys. Lett.*, 2003, **83**, (5), 966–968.
63. K. Oikawa, G. W. Qin, S. Okamoto, O. Kitakami and K. Ishida: *Appl. Phys. Lett.*, 2004, **85**, (13), 2559–2561.
64. G. W. Qin and K. Oikawa: *J. Mater. Metall.*, 2005, **4**, (2), 142–147.
65. M. R. Visokay and R. Sinclair: *Appl. Phys. Lett.*, 1995, **66**, (13), 1692–1694.
66. C. Chen, O. Kitakami, S. Okamoto and Y. Shimada: *Appl. Phys. Lett.*, 2000, **76**, (22), 3218–3220.
67. H. Yamaguchi, O. Kitakami, S. Okamoto and Y. Shimada: *Appl. Phys. Lett.*, 2001, **79**, (13), 2001–2003.
68. O. Kitakami, Y. Shimada, K. Oikawa, H. Daimon and K. Fukamichi: *Appl. Phys. Lett.*, 2001, **78**, (8), 1104–1106.
69. C. L. Platt, K. W. Wierman, E. B. Svedberg, R. van de Veerdonk, J. K. Howard, A. G. Roy and D. E. Laughlin: *J. Appl. Phys.*, 2002, **78**, (25), 6104–6109.
70. S. R. Lee, S. Yang, Y. K. Kim and J. G. Na: *Appl. Phys. Lett.*, 2001, **78**, (25), 4001–4003.
71. Y. Endo, K. Oikawa, T. Miyazaki, O. Kitakami and Y. Shimada: *J. Appl. Phys.*, 2003, **94**, (11), 7222–7226.
72. A. Martins, M. C. A. Fantini, N. M. Souza-Neto, A. Y. Ramos and A. D. Santos: *J. Magn. Magn. Mater.*, 2006, **305**, (1), 152–156.
73. Y. Zhu and J. W. Cai: *Appl. Phys. Lett.*, 2005, **87**, (3), 032504–032506.
74. S. Jeong, M. E. McHenry and D. E. Laughlin: *IEEE Trans. Magn.*, 2001, **37**, (4), 1309–1311.
75. T. Shima, K. Takanashi, Y. K. Takahashi and K. Hono: *Appl. Phys. Lett.*, 2002, **81**, (6), 1050–1052.
76. H. Zeng, M. L. Yan, N. Powers and D. J. Sellmyer: *Appl. Phys. Lett.*, 2002, **80**, (13), 2350–2352.
77. D. Suess, T. Schrefl, R. Dittrich, M. Kirschner, F. Dorfbaure, G. Hrkac and J. Fidler: *J. Magn. Magn. Mater.*, 2005, **290–291**, 551–554.
78. S. Okamoto, O. Kitakami, N. Kikuchi, T. Miyazaki, Y. Shimada and T. H. Chiang: *J. Phys., Condens. Matter*, 2004, **16**, (12), 2109–2115.
79. T. Miyazaki, O. Kitakami, S. Okamoto, Y. Shimada, Z. Akase, Y. Murakami, D. Shindo, Y. K. Takahashi and K. Hono: *Phys. Rev. B*, 2005, **72B**, (14), 144419-1-5.
80. Y. K. Takahashi, T. Koyama, M. Ohnuma, T. Ohkubo and K. Hono: *J. Appl. Phys.*, 2004, **95**, (5), 2690–2696.
81. J. W. Cahn and J. E. Hilliard: *J. Chem. Phys.*, 1959, **31**, 688–696.
82. B. Yang, M. Asta, O. N. Mryasov, T. J. Klemmer and R. W. Chantrell: *Acta Mater.*, 2006, **54**, (16), 4201–4211.
83. S. Okamoto, N. Kikuchi, O. Kitakami, T. Miyazaki, Y. Shimada and K. Fukamichi: *Phys. Rev. B*, 2002, **67B**, (2), 094422-1-7.
84. S. Takei, S. Shomura, A. Morisako, M. Matsumoto and T. Haeiwa: *J. Appl. Phys.*, 1997, **81**, (8), 4674–4676.
85. J. Sayama, K. Mizutani, T. Asahi and T. Osaka: *Appl. Phys. Lett.*, 2004, **85**, 5640–5642.
86. T. Osaka, Y. Yamashita, J. Sayama, T. Asahi, J. Ariake, K. Harada and K. Ouchi: *IEEE Trans. Magn.*, 2007, **43**, (6), 2109–2111.
87. Y. G. Ma, Z. Yang, M. Matsumoto, A. Morisako and S. Takei: *J. Magn. Magn. Mater.*, 2003, **267**, (3), 341–346.
88. T. Okumoto, K. Yamasawa, X. Liu, A. Matsumoto and A. Morisako: *IEEE Trans. Magn.*, 2005, **41**, (10), 3139–3141.

89. Y. G. Ma, Z. Yang, F. L. Wei, M. Matsumoto, A. Morisako and S. Takei: *Phys. Status Solidi A*, 2004, **201A**, (9), 2112–2118.
90. O. Chubykalo, B. Lengsfield, J. Kaufman and B. Jones: *J. Appl. Phys.*, 2002, **91**, (5), 3129–3138.
91. M. Benakli, A. F. Torabi, M. L. Mallary, H. Zhou and H. N. Bertram: *IEEE Trans. Magn.*, 2001, **37**, (4), 1564–1566.
92. H. Zhou H and H. N. Bertram: *IEEE Trans. Magn.*, 2002, **38**, (2), 1405–1421.
93. X. Z. Cheng and M. B. A. Jalil: *IEEE Trans. Magn.*, 2005, **41**, (10), 3115–3117.
94. Y. Nakamura: *J. Magn. Magn. Mater.*, 1999, **200**, 634–648.
95. Q. Peng and H. N. Bertram: *IEEE Trans. Magn.*, 1996, **32**, (5), 3566–3568.
96. J. S. Goldberg and H. Zhou: *IEEE Trans. Magn.*, 2004, **40**, (4), 2558–2560.
97. C. H. Hee, J. P. Wang, H. Gong and T. S. Low: *J. Appl. Phys.*, 2000, **87**, (9), 5535–5537; *J. Appl. Phys.*, 2001, **235**, (1–3), 440–444.
98. O. Chubykalo, B. Lengsfield and B. Jones: *IEEE Trans. Magn.*, 2001, **37**, (4), 1363–1365.
99. G. Khanna, B. M. Clemens, H. Zhou and H. N. Bertram: *IEEE Trans. Magn.*, 2001, **37**, (4), 1468–1470.
100. P. J. Grundy: *J. Phys. D*, 1998, **31D**, 2975–2990.
101. Y. J. Chen, D. Y. Dai, H. B Zhao, S. I. Pang, J. H. Yin, L. J. Wu, T. P. Guan, S. N. Piramanayagam and J. P. Wang: *Appl. Phys. A*, 2005, **81A**, (1), 147–150.
102. S. N. Piramanayagam, J. H. Yin, H. B. Zhao, J. Kasim, Y. J. Chen, J. Zhang and C. H. Hee: *Appl. Phys. Lett.*, 2003, **83**, (6), 1175–1177.
103. X. Z. Cheng and M. B. A. Jalil: *IEEE Trans. Magn.*, 2005, **41**, (10), 3115–3117.
104. Y. Y. Zou, J. P. Wang, C. H. Hee and T. C. Chong: *Appl. Phys. Lett.*, 2003, **82**, (15), 2473–2475.
105. T. J. Klemmer and K. Pelhos: *Appl. Phys. Lett.*, 2006, **88**, (16), 162507–162509.
106. M. Albrecht, G. H. Hu, I. L. Guhr, T. C. Ulbrich, J. Boneberg, P. Leiderer and G. Schatz: *Nat. Mater.*, 2005, **4**, (3), 203–206.
107. J. J. Miles: *IEEE Trans. Magn.*, 2007, **43**, (3), 955–967.
108. L. L. Lee, D. E. Laughlin and D. N. Lambeth: *IEEE Trans. Magn.*, 1994, **36**, 3951–3953.
109. S. Yoshimura, D. D. Djayaprawira, T. K. Kong, Y. Masuda, H. Shoji and M. Takahashi: *J. Appl. Phys.*, 2000, **87**, (9), 6860–6862.
110. S. N. Piramanayagam, Y. F. Xu, D. Y. Dai, L. Huang, S. I. Pang and J. P. Wang: *J. Appl. Phys.*, 2002, **91**, (10), 7685–7687.
111. N. Inaba and M. Futamoto: *IEICE Trans. Magn.*, 2000, **E83C**, 1467–1474.
112. Y. Matsuda, Y. Yahisa and J. Inagaki: *J. Appl. Phys.*, 1996, **79**, 5351–5353.
113. A. C. Sun, J. H. Hsu, C. H. Sheng, P. C. Ku and H. L. Huang: *IEEE Trans. Magn.*, 2007, **43**, (2), 882–884.
114. E. W. Soo, J. P. Wang, C. J. Sun, Y. F. Xu, T. C. Chong and G. M. Chow: *J. Magn. Magn. Mater.*, 2001, **235**, (1–3), 93–97.
115. Y. Ikeda, Y. Sonobe, G. Seltzer, B. K. Ren and P. Rice: *IEEE Trans. Magn.*, 2001, **37**, 1583–1585.
116. J. Ariake, N. Honda and K. Ouchi: *IEEE Trans. Magn.*, 2003, **39**, 2294–2296.
117. Y. Inaba, T. Shimatsu, T. Oikawa, H. Sato, H. Aoi and H. Muraoka: *IEEE Trans. Magn.*, 2004, **40**, (4), 2486–2488.
118. S. N. Piramanayagam, C. K. Pock, L. Lu, C. Y. Ong, J. Z. Shi and C. S. Mah: *Appl. Phys. Lett.*, 2006, **89**, 162504–162556.
119. S. N. Piramanayagam, J. Z. Shi, H. B. Zhao, C. K. Pock, C. S. Mah, C. Y. Ong, J. Zhang, Y. S. Kay and L. Lu: *IEEE Trans. Magn.*, 2007, **43**, (2), 633–638.
120. S. N. Piramanayagama and K. Srinivasan: *Appl. Phys. Lett.*, 2007, **91**, (14), 142508–142510.
121. J. G. Zhu and Y. Tang: *J. Appl. Phys.*, 2006, **99**, 08Q903-1-3.
122. Y. Tang and J. G. Zhu: *IEEE Trans. Magn.*, 2006, **42**, (10), 2360–2362.
123. D. Suess, J. Fidler, K. Porath, T. Schrefl and D. Weller: *J. Appl. Phys.*, 2006, **99**, 08G905-1-3.
124. J. G. Zhu and Y. Tang: *IEEE Trans. Magn.*, 2007, **43**, (2), 687–692.
125. D. E. Laughlin, Y. Peng, Y. Qin, M. Lin and J. G. Zhu: *IEEE Trans. Magn.*, 2007, **43**, (2), 693–697.
126. Y. L. Qin, D. E. Laughlin, Y. Peng and J. G. Zhu: *IEEE Trans. Magn.*, 2007, **43**, (6), 2136–2138.
127. A. C. Sun, J. H. Hsu, P. C. Kuo and H. L. Huang: *IEEE Trans. Magn.*, 2007, **43**, (6), 2130–2132.
128. M. T. Rahman, N. N. Shams, Y. C. Wu and C. H. Lai: *Appl. Phys. Lett.*, 2007, **91**, 132505-1-3.
129. S. Y. Chou and P. R. Krauss: *J. Magn. Magn. Mater.*, 1996, **155**, (1–3), 151–153.
130. R. L. White, R. M. H. New and R. F. W. Pease: *IEEE Trans. Magn.*, 1997, **33**, (1), 990–995.
131. C. Chappert, H. Bernas, J. Ferre, V. Kottler, J. P. Jamet, Y. Chen, E. Cambril, T. Devolder, F. Rousseaux, V. Mathet and H. Launois: *Science*, 1998, **280**, (5371), 1919–1922.
132. Y. Soeno, M. Moriya, K. Ito, K. Hattori, A. Kaizu, T. Aoyama, M. Matsuzaki and H. Sakai: *IEEE Trans. Magn.*, 2003, **39**, 1967–1969.
133. J. Lohau, A. Moser, C. T. Rettner, M. E. Best and B. D. Terris: *Appl. Phys. Lett.*, 2001, **78**, 990–992.
134. B. D. Terris and T. Thomson: *J. Phys. D*, 2005, **38D**, 199–222.
135. H. J. Richter, A. Y. Dobin, O. Heinonen, K. Z. Gao, R. J. M. van de Veerdonk, R. T. Lynch, J. Xue, D. Weller, P. Asselin, M. F. Erden and R. M. Brockie: *IEEE Trans. Magn.*, 2006, **42**, (10), 2255–2260.
136. M. Albrecht, S. Ganesan, C. T. Rettner, A. Moser, M. E. Best, R. L. White and B. D. Terris: *IEEE Trans. Magn.*, 2003, **39**, 2323–2325.
137. J. I. Martin, J. Nogues, K. Liu, J. L. Vicent and I. K. Schuller: *J. Magn. Magn. Mater.*, 2003, **256**, 449–501.
138. T. Thurn-Albrecht, J. Schotter, C. A. Kastle, N. Emley, T. Shibauchi, L. Krusin-Elbaum, K. Guarini, C. T. Black, M. T. Tuominen and T. P. Russell: *Science*, 2000, **290**, 2126–2129.
139. H. Masuda, H. Yamada, M. Satoh, H. Asoh, M. Nakao and T. Tamamura: *Appl. Phys. Lett.*, 1997, **71**, 2770–2772.
140. C. Haginoya, K. Koike, Y. Hirayama, J. Yamamoto, M. Ishibashi, O. Kitakami and Y. Shimada: *Appl. Phys. Lett.*, 1999, **75**, (20), 3159–3161.
141. S. H. Sun, C. B. Murray, D. Weller, L. Folks and A. Moser: *Science*, 2000, **287**, 1989–1992.
142. X. C. Sun, S. S. Kang, J. W. Harrell, D. E. Nikles, Z. R. Dai, J. Li and Z. L. Wang: *J. Appl. Phys.*, 2003, **93**, (10), 7337–7339.
143. S. Kang, J. W. Harrell and D. E. Nikles: *Nano Lett.*, 2002, **2**, (10), 1033–1036.
144. S. S. Kang, Z. Y. Jia, D. E. Nikles and J. W. Harrell: *IEEE Trans. Magn.*, 2003, **39**, (5), 2753–2757.
145. Q. Y. Yan, T. Kim, A. Purkayastha, P. G. Ganesan, M. Shima and G. Ramanath: *Adv. Mater.*, 2005, **17**, (8), 2233–2237.
146. H. L. Nguyen, L. E. M. Howard, G. W. Stinton, S. R. Giblin, B. K. Tanner, I. Terry, A. K. Hughes, I. M. Ross, A. Serres and J. S. O. Evans: *Chem. Mater.*, 2006, **18**, (26), 6414–6424.
147. C. B. Rong, D. R. Li, V. Nandwana, N. Poudyal, Y. Ding, Z. L. Wang, H. Zeng and J. P. Liu: *Adv. Mater.*, 2006, **18**, (22), 2984–2989.
148. U. Wiedwald, A. Klimmer, B. Kern, L. Han, H. G. Boyen, P. Ziemann and K. Fauth: *Appl. Phys. Lett.*, 2007, **90**, (6), 062508-1-3.
149. J. W. Harrell, S. Kang, Z. Jia, D. E. Nikles, R. Chantrell and A. Satoh: *Appl. Phys. Lett.*, 2005, **87**, (20), 202508–202510.
150. J. M. Qiu, J. M. Bai and J. P. Wang: *Appl. Phys. Lett.*, 2006, **89**, (22), 222506-1-3.
151. H. Kodama, S. Momose, N. Ihara, T. Uzumaki and A. Tanaka: *Appl. Phys. Lett.*, 2003, **83**, (25), 5253–5255.
152. C. Kim, T. Loedding, S. Jang, H. Zeng, Y. Sui and D. J. Sellmyer: *Appl. Phys. Lett.*, 2007, **91**, 172508-1-3.
153. T. W. McDaniel, W. A. Challener and K. Sendur: *IEEE Trans. Magn.*, 2003, **39**, (4), 1972–1979.
154. H. Katayama, S. Sawamura, Y. Ogimoto, J. Nakajima, K. Kojima and K. Ohta: *J. Magn. Soc. Jpn*, 1999, **23**, 233–234.
155. T. McDaniel and R. Victora (eds.): 'Handbook of magneto-optical data recording'; 1997, Park Ridge, NJ, Noyes-Andrews.
156. M. Mansuripur: 'The physical principles of magneto-optical recording'; 1995, Cambridge, Cambridge University Press.
157. S. M. Mansfield and G. S. Kino: *Appl. Phys. Lett.*, 1990, **57**, 2615–2617; B. D. Terris, H. J. Mamin and D. Rugar: *Appl. Phys. Lett.*, 1996, **68**, 141–143.
158. H. Bethe: *Phys. Rev.*, 1944, **66**, 163–167.
159. T. Suzuki, I. Yusuke, M. Birukawa and W. van Drent: *IEEE Trans. Magn.*, 1998, **34**, 399–403.
160. L. Yin, V. K. Vlasko-Vlasov, A. Rydh, J. Pearson, U. Welp, S.-H. Chang, S. K. Gray, G. C. Schatz, D. B. Brown and C. W. Kimball: *Appl. Phys. Lett.*, 2004, **85**, (3), 467–469.
161. E. Popov, N. Bonod, M. Neviere, H. Rigneault, P.-F. Lenne and P. Chaumet: *Appl. Opt.*, 2005, **44**, 2332–2337.
162. X. Shi and L. Hesselink: *Jpn J. Appl. Phys.*, 2001, **41**, 1632–1635.
163. K. W. Ng, S. H. Leong, Z. Yuan, B. Liu and Y. Ma: *Appl. Phys. Lett.*, 2007, **91**, (17), 172511-1-3.

164. H. Tian, C.-Y. Cheung, P.-K. Wang and K. Chung: *IEEE Trans. Magn.*, 1997, **33**, 3130–3132.
165. Y. Sonobe, D. Weller, Y. Ikeda, K. Takano, M. E. Schabes, G. Zeltzer, H. Do, B. K. Yen and M. E. Best: *J. Magn. Magn. Mater.*, 2001, **235**, (1–3), 424–428.
166. Y. Sonobe, H. Muraoka, K. Miura, Y. Nakamura, K. Takano, A. Moser, H. Do, B. K. Yen, Y. Ikeda, N. Supper and W. Weresin: *IEEE Trans. Magn.*, 2002, **38**, (4), 1632–1636.
167. Y. Sonobe, H. Muraoka, K. Miura, Y. Nakamura, K. Takano, A. Moser, H. Do, K. Yen, Y. Ikeda and N. Supper: *J. Appl. Phys.*, 2002, **91**, 8055–8057.
168. J. H. Judy: *J. Magn. Magn. Mater.*, 2005, **287**, 16–26.
169. O. Kitakami, T. Shimatsu and H. Muraoka: *Jpn J. Appl. Phys.*, 2002, **41**, 455–457.
170. A. Y. Dobin and H. J. Richter: *J. Appl. Phys.*, 2007, **101**, (9), 09K108-1-3.
171. J. P. Wang, W. K. Shen and S. Y. Hong: *IEEE Trans. Magn.*, 2007, **43**, (2), 682–686.
172. A. Y. Dobin and H. J. Richter: *Appl. Phys. Lett.*, 2006, **89**, (6), 062512-1-3.
173. H. Gavrila: *J. Opt. Adv. Mater.*, 2006, **8**, (2), 449–454.
174. R. H. Victora and X. Shen: *IEEE Trans. Magn.*, 2005, **41**, (10), 2828–2831.
175. J. P. Wang, W. K. Shen and J. M. Bai: *IEEE Trans. Magn.*, 2005, **41**, (10), 3181–3186.